Data-driven Cross-lingual Syntax: An Agreement Study with Massively Multilingual Models

Andrea Gregor de Varda
University of Milano-Bicocca
a.devarda@campus.unimib.it

Marco Marelli
University of Milano-Bicocca
m.marelli@unimib.it

Massively multilingual models such as mBERT and XLM-R are increasingly valued in Natural Language Processing research and applications, due to their ability to tackle the uneven distribution of resources available for different languages. The models' ability to process multiple languages relying on a shared set of parameters raises the question of whether the grammatical knowledge they extracted during pre-training can be considered as a data-driven cross-lingual grammar. The present work studies the inner workings of mBERT and XLM-R in order to test the cross-lingual consistency of the individual neural units that respond to a precise syntactic phenomenon, that is, number agreement, in five languages (English, German, French, Hebrew, Russian). We found that there is a significant overlap in the latent dimensions that encode agreement across the languages we considered. This overlap is larger (a) for long- vis-à-vis short-distance agreement and (b) when considering XLM-R as compared to mBERT, and peaks in the intermediate layers of the network. We further show that a small set of syntax-sensitive neurons can capture agreement violations across languages; however, their contribution is not decisive in agreement processing.

1. Introduction

Massively multilingual models (MMMs) such as multilingual BERT (mBERT, Devlin et al. 2019) and XLM-RoBERTa (XLM-R, Conneau et al. 2020a) are transformer-based language representation models trained simultaneously on multilingual text in several languages (104 and 100, respectively). They do not involve any architectural changes with respect to their monolingual counterparts (BERT and RoBERTa), nor any reliance on any explicit cross-lingual signal. MMMs reach impressive performance scores in tasks involving zero-shot cross-lingual transfer, a procedure that entails the fine-tuning of the model on supervised data in a language L_1 and its application to a different

Action Editor: Byron Wallace. Submission received: 27 June 2022; revised version received: 24 September 2022; accepted for publication: 12 October 2022.

https://doi.org/10.1162/coli_a_00472

language L_2, with no additional training.[1] This procedure has been shown to be successful across a variety of languages and downstream tasks (Pires, Schlinger, and Garrette 2019; Wu and Dredze 2019; Dufter and Schütze 2020; Liu et al. 2020; Lauscher et al. 2020; see Doddapaneni et al. 2021 for a review). Although performance levels tend to be positively correlated with the typological similarity between the two languages (Lauscher et al. 2020), zero-shot cross-lingual transfer yields surprising results in languages written in different scripts (Pires, Schlinger, and Garrette 2019) and with little or no (Karthikeyan et al. 2020); (Conneau et al. 2020b) vocabulary overlap. With only a subset of the world's languages being properly represented in the evolving language technologies, the distribution of resources available for NLP researchers is extremely asymmetrical (Joshi et al. 2020). Massively multilingual models represent an attempt to temper the effects of this imbalance by exploiting the knowledge that can be shared across languages.

The performance of MMMs in the transfer tasks hints at the possibility that their internal representations might be inherently cross-lingual (Pires, Schlinger, and Garrette 2019; Dufter and Schütze 2020; Guarasci et al. 2022). Dufter and Schütze (2020) argue that mBERT multilingualism might be due to its finite number of dimensions, which forces it to exploit common structures to compress representations across languages. The question of whether a multilingual model induces a shared representational space where abstract cross-linguistic regularities are encoded through a common set of parameters is remindful of the debate on the neural underpinning of linguistic knowledge in multilingual individuals (see Dhar and Bisazza [2021] for similar considerations). In particular, the problem is reminiscent of the question of whether the neural resources allocated to different languages in a multilingual brain overlap (at least partially, see Perani et al. 1998; Abutalebi, Cappa, and Perani 2001; Perani and Abutalebi 2005; Green 2008) or involve functionally independent neural populations (Kim et al. 1997; Tham et al. 2005; Tan et al. 2011; Xu et al. 2017). If we consider the possibility of looking at artificial neural networks as a different "species" (Cummins and Schwarz 1988; McCloskey 1991), in a fashion that reminds us of the study of animal models, the study of the representations produced by these networks might offer novel insights into the space of possible solutions to the cognitive question mentioned above.

A modest but increasing number of findings is contributing to the question of whether MMMs develop a data-driven universal grammar through an analysis of their internal states. A study targeting mBERT vector representations has shown that syntactic trees can be retrieved from its intermediate representational subspaces, with these subspaces being approximately shared across languages (Chi, Hewitt, and Manning 2020). These intermediate subspaces can be used in machine translation, by identifying the nearest neighbor in different representation spaces given a sentence in a source language and a set of candidates in a target language (Pires, Schlinger, and Garrette 2019). Other studies have performed representational similarity analysis comparing encoded sentences in different languages; while most results suggested that MMMs develop a cross-lingual space in the intermediate layers (Conneau et al. 2020b; Del and Fishel 2021; Muller et al. 2021), as shown by converging similarity between sentence representations in deeper layers of the networks, contrasting results have documented an opposed pattern when sentence representations are obtained through CLS pooling instead of mean-pooling (Singh et al. 2019, although see Del and Fishel 2021 for a case against the CLS pooling strategy).

1 Where L_1 and L_2 are typically a resource-rich and resource-poor language, respectively.

The work we reviewed insofar targeted vector representations as a whole, neglecting the role of the individual parameters in the embeddings. However, while research in NLP used to largely overlook the single dimensions in the neural representations, a recent research line is starting to investigate the linguistic properties encoded in individual neurons and attention weights (see for instance Karpathy, Johnson, and Fei-Fei 2015; Li et al. 2015; Radford, Jozefowicz, and Sutskever 2017; Tang et al. 2017; Kementchedjhieva and Lopez 2018; Bau et al. 2018; Dalvi et al. 2019a; Lakretz et al. 2019; Pinter, Marone, and Eisenstein 2019; Serrano and Smith 2019). Aiming to extend this line of analysis to a multilingual setting, we isolated the contribution of the individual neurons in mBERT and XLM-R, defined as dimensions in the deep latent representations. While most studies assessing the models' cross-lingualism considered phrasal representations as a whole, without discerning between semantic and syntactic properties (Pires, Schlinger, and Garrette 2019; Liu et al. 2020; Del and Fishel 2021), we restricted our study to number agreement, a structure-dependent phenomenon. It has been shown that BERT captures syntactic features in the intermediate $[\![6, 9]\!]$ layers (Jawahar, Sagot, and Seddah 2019), which are the same that show the highest representational similarity across languages in the multilingual model (Del and Fishel 2021). This layer-wise convergence of syntactic and cross-lingual knowledge in (m)BERT inspired our choice to constrain our study to a structural linguistic feature. The general question of whether MMMs represent patterns that generalize across languages is hereby framed as an inquiry into the cross-lingual stability of the neural units that encode number agreement.

2. Related Work

A productive research line in computational linguistics has focused on the analysis of the linguistic features learned by neural language models. This line of analysis aimed at testing whether sequence processing networks were able to construct hierarchical representations of the linguistic input, or either relied on local heuristics without acquiring core knowledge of different grammatical phenomena. A popular trend within this framework relied on the large-scale unsupervised training of a language model, and the fine-grained evaluation of the probabilities it assigned to different linguistic units in a controlled setting as a "behavioral" correlate of its ability to capture the regularities of a given language. Along this line of work, numerous studies have used long-distance number agreement as a way of probing the networks' ability to encode structure-dependent relationships (Linzen, Dupoux, and Goldberg 2016; Bernardy and Lappin 2017; Gulordava et al. 2018; Kuncoro et al. 2018; Marvin and Linzen 2018; Goldberg 2019; van Schijndel, Mueller, and Linzen 2019; Lasri, Lenci, and Poibeau 2022). While all the previous studies evaluated the models on their native tasks, Lakretz et al. (2019) presented an ablation-based study of the inner mechanisms that underlie number agreement processing in LSTMs at the single neuron level, showing that a very sparse set of specialized units carried number features from the subject to the verb across the intervening material. In a similar vein, Finlayson et al. (2021) have used causal analysis to implicate specific neurons in transformer models.

With the debut of multilingual models, the previous studies were replicated in different languages, showing that mBERT successfully captures syntax-sensitive agreement patterns (Bacon and Regier 2019; Mueller et al. 2020). However, these experiments limited their focus on the analysis of mBERT's predictive behavior, overlooking the functioning of its internal processes. A complementary line of analysis has investigated

how multilingual models encode other linguistic attributes in their internal representations. For instance, Gonen, Ravfogel, and Goldberg (2022) have shown that gender information is encoded in both language-specific and language-neutral subspaces in the embeddings of mBERT. Furthermore, Antverg and Belinkov (2021) have investigated the cross-lingual consistency in the units of mBERT and XLM-R that responded to different morphological features, showing that there is a significant overlap in the latent dimensions that encode attributes such as gender, tense, and number. Similarly, Stanczak et al. (2022) have probed the same models in 43 languages, and on a variety of morphosyntactic categories. However, while these two studies have investigated the encoding of *number* in MMMs, they have not investigated *number agreement*, that is, the structural relationship that is instantiated between a subject and a verb in a well-formed sentence. To fill this research gap, we tested whether the processes that underpin number agreement computation across languages could be ascribed to an overlapping set of latent dimensions in the structural embeddings of the models.

3. Materials and Methods

3.1 Language Models

Our experiments were performed utilizing the native masked language modeling component of mBERT and XLM-R. The configurations of the models were left unaltered with respect to their original releases (Devlin et al. 2019; Conneau et al. 2020a). In particular, we relied on the multilingual version of $\text{BERT}_{\text{BASE}}$ (cased) and on $\text{XLM-R}_{\text{BASE}}$. The two networks share an analogous structural configuration: They are composed of 12 layers, 12 self-attention heads, and a hidden size of 768. However, while mBERT is jointly trained with a masked language modeling and a next sentence prediction (NSP) objective, XLM-R drops the latter component, and increases the amount of training data. The networks did not undergo any fine-tuning nor adaptation process, as they were used as out-of-the-box masked language models. We did not mask any word throughout this work.

3.2 Materials

The agreement data was obtained from the CLAMS dataset[2] (Mueller et al. 2020), a cross-linguistic resource for the syntactic evaluation of word prediction models. CLAMS comprises subject-verb agreement challenge sets for English, German, French, Russian, and Hebrew, constructed by means of artificial grammars. Note that in abstract terms these languages encode agreement patterns in a similar way, that is, through a form of morphological inflection that links subject and verb on account of their grammatical number. For the sake of simplicity, out of the seven syntactic constructions covered in the original dataset we only included simple agreement and long-distance VP-coordination (henceforth short- and long-distance agreement; see Figure 1). We selected these two conditions as they represent the settings with the shortest and the longest dependency length between the subject and the verb, respectively. While in short-distance agreement the two constituents are immediately adjacent, in long-distance

2 Publicly available at `https://github.com/aaronmueller/clams`.

(1) (a) The author smiles
(b) *The author smile

(2) (a) The author knows many different foreign languages and likes to watch television shows
(b) *The author knows many different foreign languages and like to watch television shows

Figure 1
English examples of grammatical (a) and ungrammatical (b) sentences in the simple agreement (1) and long-distance VP-coordination (2) conditions.

agreement they are separated by a large amount of intervening verbal material (namely, the VP projection of the main phrase and the coordinating conjunction).

3.3 Procedure

In order to identify the most relevant units with respect to the agreement task, we adopted the Linguistic Correlation Analysis (LCA) procedure (Dalvi et al. 2019a,b), a supervised method based on linear classification. The first step of LCA consists of extracting the neuron activations from the model in response to the input words. Then, a logistic classifier is trained to predict a label (in our case, the grammaticality of the sentence obtained by including the word in the phrasal context) from the overall internal state of the model, with cross-entropy loss and elastic net regularization as additional loss term (Zou and Hastie 2005), with $\lambda_1 = \lambda_2 = 0.001$. The trained weights of the classifier are used as a measure of the relevance of the corresponding units with respect to the linguistic property being investigated (i.e., the binary label of grammatical acceptability); this allows sorting the neurons according to the absolute value of their respective weights. In our study, we restricted our analyses to the activations in response to the verb that should instantiate an agreement relationship with the subject (e.g., *smiles*/**smile*, *likes*/**like* in Figure 1). As a result of this choice, we trained the logistic classifiers with the verb representations as input. In the case of multi-token verbs, the activations corresponding to the two tokens were averaged, following Dalvi et al. (2019a).

Probing classifiers have the undeniable advantage of being a flexible analysis technique that can help researchers understand the roles and dynamics of the hidden components of a network and diagnose potential problems (Alain and Bengio 2016). However, several shortcomings of probing classifiers have been highlighted in the literature. For instance, it has been emphasized that the probing framework might highlight correlations between the representations generated by a language model and a given linguistic property, but it does inform us on the role of this property in the predictions of the model (Belinkov and Glass 2019; Belinkov 2022). Antverg and Belinkov (2021) have proposed a methodology to rank individual neurons in language models without the need for an external probe. This procedure involves the computation of the average network activation q(z) for every categorical label $z \in Z$; then, a simple element-wise subtraction between the centroids of each category is calculated to assess the differential role of each neuron across classes. The ranking is then obtained by sorting the neurons according to their absolute value in the vector difference. It has been shown that probe-free rankings better identify neural units that are actually used by the language models, as demonstrated through selective interventions (Antverg and Belinkov 2021). In

order to complement the results we obtained with the linear probing, and to offset the limitations that are inherent in the probing framework, we also experiment with such a **probeless** method.[3]

The ranking processes were performed independently for (a) each ranking method (linear and probeless), (b) each model (mBERT and XLM-R), (c) each agreement condition (long- and short-distance), and (d) each individual language considered, in a $2 \times 2 \times 2 \times 5$ design which allowed us to derive 40 distinct rankings. In all cases, the classifier was trained and tested on two subsets of the original data (80% train, 20% test). In order to license meaningful comparisons on the performances of the classifiers across languages, we downsampled all the short-distance challenge sets to 280 items (224 in the training and 56 in the test set), and the long-distance datasets to 800 items (640 training, 160 test). All the procedures described above were implemented with the `NeuroX` toolkit (Dalvi et al. 2019b), a Python package to perform interpretation and analysis of deep neural networks.

Once the neuron ranking was obtained, we evaluated the cross-lingual consistency in the set of neural units computing agreement across languages. In order to do so, we assessed the intersection between the top 100 neurons independently selected in each language.[4] In practice, we did not test the statistical significance of the cross-lingual overlap at the level of the whole architecture, since the estimate of our test would have been biased by the sequential flow of information within the network. The cross-lingual congruence of the neural units processing syntactic agreement could be overestimated if one does not take into account the fact that similar processes with a comparable degree of structural abstraction are likely to be processed in the same layers. Intuitively, a dimension in the first layer of XLM-R or mBERT embeddings is less likely to occupy a high position in the neuron ranking, since it is already known that syntactic features are processed in the intermediate layers of the architecture (Jawahar, Sagot, and Seddah 2019); because the probability associated with a given size of a set intersection is critically dependent on the size of the population from which the sets are sampled, a conservative approach to avoid a type-1 error is to consider a single layer as the reference population. Thus, we previously searched for the layers that were more relevant in the computation of cross-lingual agreement, and then evaluated the cross-lingual overlap in the within-layer neural population. The statistical significance of the resulting intersection size was computed through the super exact test (Wang, Zhao, and Zhang 2015), a procedure for computing the distributions of multi-set intersections based upon combinatorial theory.

4. Results

4.1 Layer-wise Analyses

In order to restrict our intersection analysis to a pre-specified layer, we first analyzed the performance of a classifier trained to predict the grammaticality label in response to each layer's activation. The results are summarized in Figure 2. In the case of mBERT,

3 We thank an anonymous reviewer for the suggestion.

4 We considered 100 units as Antverg and Belinkov (2021); however, following an anonymous reviewer's suggestion, we analyzed post hoc the ratio of weight mass that could be ascribed to these neurons. The top 100 units contribute to a substantial proportion of the weight mass of the layer (on average 45.46%), while constituting only the 13.02% of the layer units (N = 768). We report a detailed analysis in Appendix 1.

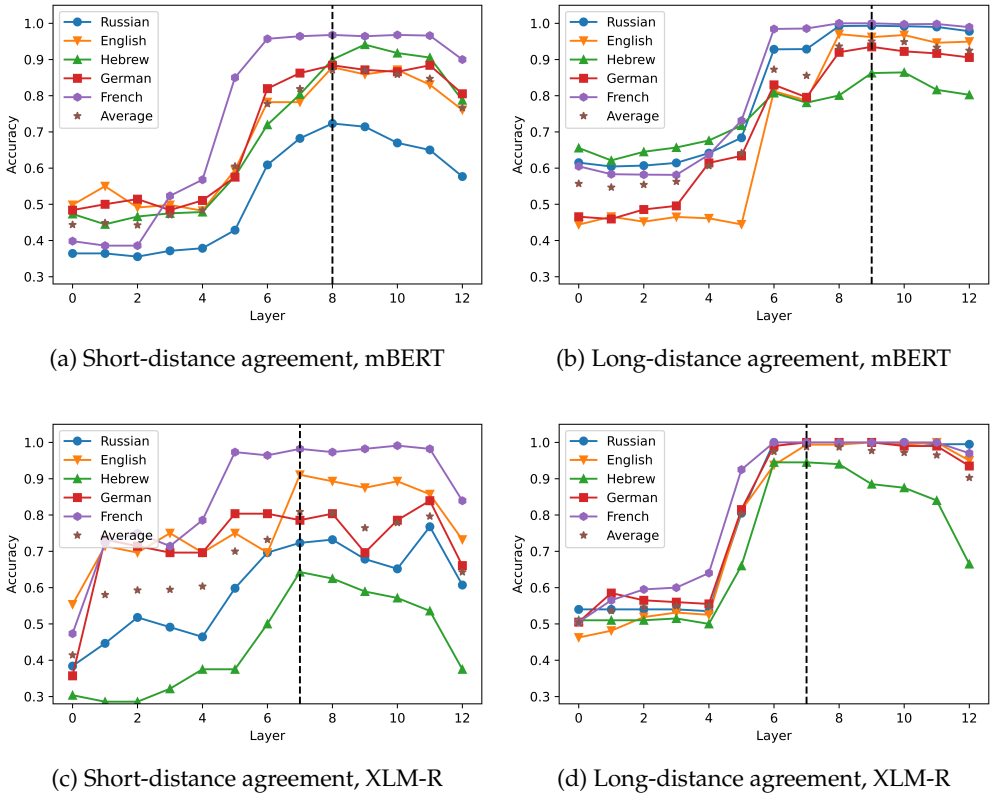

(a) Short-distance agreement, mBERT

(b) Long-distance agreement, mBERT

(c) Short-distance agreement, XLM-R

(d) Long-distance agreement, XLM-R

Figure 2
Layer-wise performance of the logistic classifier. The layer 0 includes the embedding layer representations. The vertical dashed line indicates the peak of the average accuracy obtained by the classifiers in the five languages considered.

the highest average accuracy scores in the short- (2a) and the long-distance (2b) conditions were obtained from the activations of the eighth (0.8707) and ninth (0.9505) layer, respectively. XLM-R showed a higher degree of congruence across conditions, since the highest scores were obtained in the seventh layer both in the short- (0.8089, 2c) and in the long-distance datasets (0.98775, 2d). A clear pattern that emerges from the graphs is that the accuracy curve is highly dependent on the language considered. In the case of short-distance agreement, mBERT's performance in Russian falls 0.1474 points below the average; in the long-distance condition, the performance levels in Hebrew is 0.0880 points lower than the mean. The classifiers built upon the XLM-R representations perform consistently worse in Hebrew, where their performance levels are 0.1661 and 0.0420 points below average in the short- and in the long-distance conditions, respectively. These results corroborate the finding that mBERT does not learn equally high-quality representations for its 104 languages (Wu and Dredze 2020), and extends this observation to XLM-R. The relatively poor performance scores obtained in Hebrew and Russian are also consistent with the results of the standard predictive tests obtained by Mueller et al. (2020), where mBERT's accuracy in the agreement tasks was noticeably lower in the two languages written in non-Latin scripts. Nonetheless, the *pattern* of performance across layers seems to be stable across languages and models: predictably, the activations extracted from the most shallow layers are not a solid basis

for the detection of grammatical violations; the classification accuracy increases in the intermediate layers of the network, and declines in the deepest layers.

4.2 Intersections

4.2.1 Linguistic Correlation Analysis Rankings. Building upon these results, we confined our multi-set intersection analyses to the layers that achieved the best results in the classification task, namely, the seventh layer for XLM-R, and the eighth and the ninth layer for mBERT (short- and long-distance agreement, respectively). The results of the super exact test on the cross-lingual neural overlap are depicted in Figure 3, and

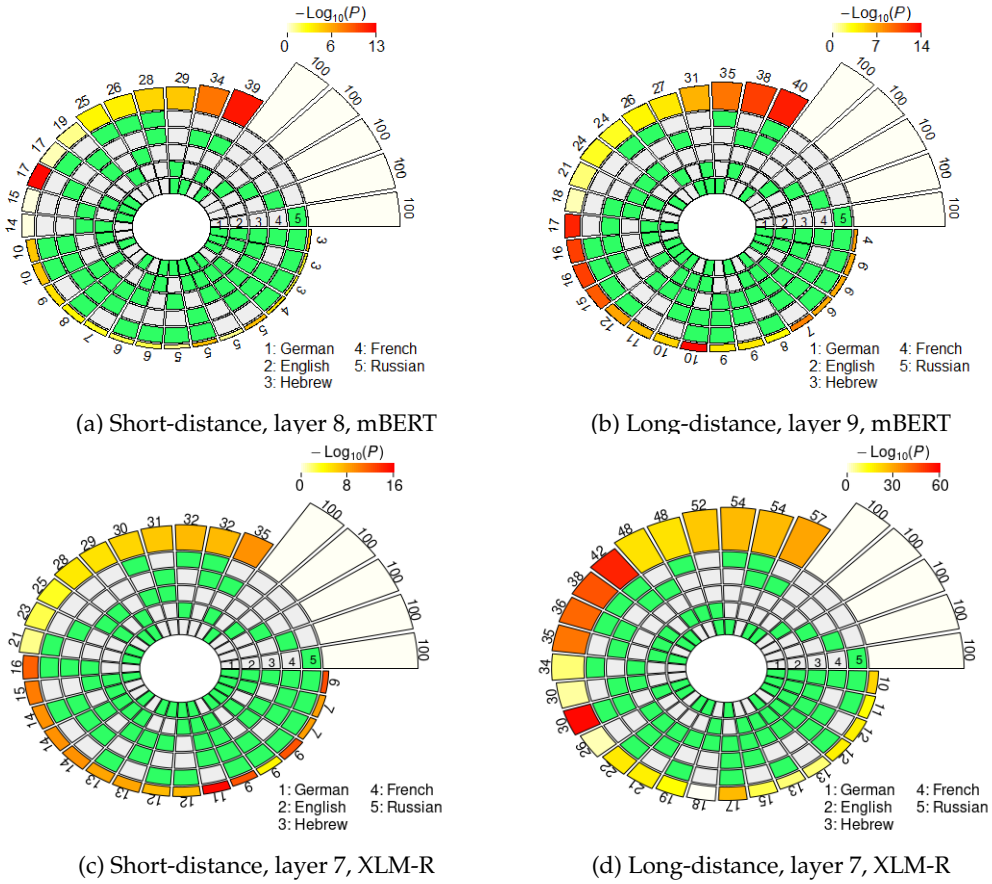

(a) Short-distance, layer 8, mBERT

(b) Long-distance, layer 9, mBERT

(c) Short-distance, layer 7, XLM-R

(d) Long-distance, layer 7, XLM-R

Figure 3
Set intersections of the top 100 neural units responsible for subject-verb agreement in the two conditions. The five concentric rings in the middle represent the five sets of top neurons relative to each language, and the individual sections indicate the presence (green) or the absence (grey) of the sets in each intersection. Each circular sector corresponds to a particular configuration of set intersections. For instance, a sector with the first and the last segment highlighted in green corresponds to the German ∩ Russian intersection. The height of the bars in the outer layer is proportional to the intersection sizes, which are made explicit by the numbers on the top. The color intensity of the bars represents the log-transformed p-value significance of the intersections, as computed with the super exact test. The white bars on the right of the diagrams are not associated with *FE* and statistical significance, and they simply report the number of considered units for each language (N = 100). The segments are ordered counterclockwise by intersection size.

reported in detail in Appendix 2 (Tables 2, 3 for mBERT; Tables 4, 5 for XLM-R). All two-, three-, four-, and five-way combinations show an overrepresentation of the set intersection relative to the random expectation. This overrepresentation is statistically significant in all but four intersections (out of 104); in the case of mBERT, the statistical significance of the fold enrichment (*FE*; i.e., the ratio between observed and expected overlap[5]) exceeds the conventional threshold of $\alpha = .05$ in the En[6] $\cap$ He and De $\cap$ He cases in the short-distance condition, and He $\cap$ Fr in the long-distance condition. The only combination with $p > .05$ in the intersections based on XLM-R is En $\cap$ He; notably, Hebrew is present in all the non-significant intersections.

In the case of the mBERT short-distance agreement results, the two-, three-, and four-way intersections associated with the highest fold enrichment are En $\cap$ Fr, En $\cap$ Fr $\cap$ Ge, and En $\cap$ Fr $\cap$ De $\cap$ Ru, respectively (see Figure 3a). These three combinations have in common the absence of the Hebrew set, and the presence of the English and the French sets. On average, the pairwise set intersections in the case of short-distance agreement comprise 24.9 units; a striking number of 39 units is found in the En $\cap$ Fr intersection ($FE = 2.9952$, $p = 5.84 \cdot 10^{-13}$). Remarkably, three neurons survived all the five-way set intersections, occupying a high position in all the five language-specific rankings ($FE = 104.3677$, $p = 3.39 \cdot 10^{-6}$). In the case of long-distance agreement, the highest fold enrichment for each $N_{2\ldots4}$-way intersection is found in Fr $\cap$ Ru, Fr $\cap$ En $\cap$ Ge, and Fr $\cap$ En $\cap$ De $\cap$ Ru, with Hebrew being again the absent language in the three combinations and French appearing in all of them (see Figure 3b). The average pairwise intersection size is 28.4; the five-way intersection in the long-distance condition includes four neurons, with $FE = 139.1569$ and $p = 1.01 \cdot 10^{-10}$. Overall, agreement-related information displays a greater degree of convergence in the long- vis-à-vis the short-distance condition. Indeed, in the former case intersection sizes are consistently bigger, and associated with higher FE (on average, the *FE* for the pairwise intersections is 1.8893 in the short-distance condition, and 2.1811 in the long-distance condition).

The results obtained by XLM-R mirror the ones derived from mBERT: Long-distance agreement is characterized by larger intersections in the top-100 neuron rankings, showing signs of a stronger cross-lingual alignment. Indeed, the average pairwise *FE* is 2.1965 in the short-distance condition, and 3.3333 in the long-distance condition. The $N_{2\ldots4}$-way intersections with highest *FE* in the short-distance condition are En $\cap$ Fr, He $\cap$ Fr $\cap$ Ru, and De $\cap$ En $\cap$ Fr $\cap$ Ru (see Figure 3c); in the long-distance condition, the combinations that share the highest number of neurons are De $\cap$ Fr, De $\cap$ Fr $\cap$ Ru, and De $\cap$ En $\cap$ Fr $\cap$ Ru (see Figure 3d). While Hebrew appears in one top combination in the short-distance condition, most of the best scoring intersections do not include it. The number of neurons that are present in the top-100 sets across all five languages is remarkably high: In the short-distance condition, we found six cross-lingual neurons ($FE = 208.7354$, $p = 3.87 \cdot 10^{-13}$), whereas in the long-distance condition the number rises to ten ($FE = 347.8924$, $p = 1.29 \cdot 10^{23}$, by far the highest *FE* score we obtained in our study). The overall congruence in the neural units responding to agreement violations is stronger in XLM-R with respect to mBERT; this disparity is particularly evident in the long-distance condition, where the neurons surviving through the five-way intersection are more than double.

5 With the observed overlap being equal, higher-degree set intersections—which have lower expected overlap—will have higher FE.

6 For readability purposes, the set of the top 100 units selected for a given language is reported with the ISO 639-1 code of that language (English: En; German: De; Russian: Ru; French: Fr; Hebrew: He).

4.2.2 Probeless Rankings. As with the LCA method, we restricted our multi-set analyses to the individual units populating the seventh layer in the case of XLM-R, and the eighth and ninth layers for mBERT (long- and short-distance agreement). The results of the super exact test based on the probeless rankings are graphically depicted in Figure 4, and reported in detail in Appendix 2 (Tables 6, 7 for mBERT; Tables 8, 9 for XLM-R). From a qualitative standpoint, the results obtained with the probeless ranking method are analogous to those described in the previous section. Intersection sizes show a general overrepresentation of units with respect to what would be expected by chance; indeed, when considering short-distance agreement, in all the set intersections the size of the observed overlap exceeds the size of the expected overlap by a significant margin with the exception of very few combinations, most of which include the Hebrew set (mBERT: En ∩ He; XLM-R: Fr ∩ Ru, He ∩ Fr, En ∩ He, De ∩ He, De ∩ He ∩ Ru, De ∩ He ∩ Fr). In the long-distance condition there are no exceptions to this trend, with the

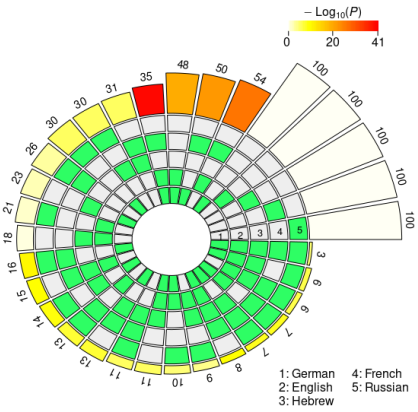

(a) Short-distance, layer 8, mBERT

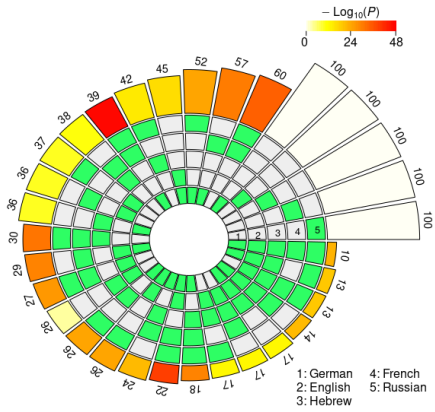

(b) Long-distance, layer 9, mBERT

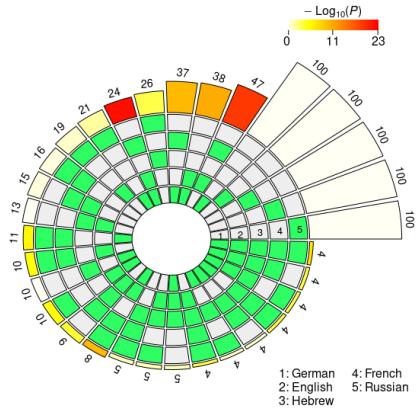

(c) Short-distance, layer 7, XLM-R

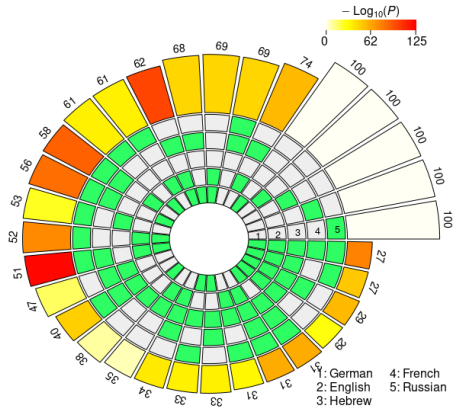

(d) Long-distance, layer 7, XLM-R

Figure 4
$N_{2\ldots5}$-way intersection statistics derived from the rankings obtained with the probeless method.

FE associated with all intersections being statistically significant, regardless of model type. Once again, intersection sizes tend to be bigger in the long-distance condition, showing signs of a stronger representational alignment across languages. Restricting our focus to pairwise overlap, the average *FE* is higher in the long-distance intersection data (mBERT, short: 2.7421; mBERT, long: 3.2947; XLM-R, short: 1.8586; XLM-R, long: 4.416). Furthermore, the cross-lingual overlap is more pronounced when considering the embeddings of the RoBERTa-based encoder (see above), in line with the LCA-based results.

In the case of mBERT, the intersections with the highest overrepresentation of the fold for each degree are En ∩ Fr, En ∩ Fr ∩ De, En ∩ Fr ∩ De ∩ He (short-distance), and Fr ∩ Ru, Fr ∩ Ru ∩ De, Fr ∩ Ru ∩ De ∩ En (long-distance). In the case of XLM-R, the intersections with the highest *FE* are En ∩ Fr, En ∩ Fr ∩ De, En ∩ Fr ∩ De ∩ Ru (both long- and short-distance). While Hebrew appears in one top combination in the short-distance condition (mBERT), all the other best scoring intersections do not include it; on the other hand, they all include the French set, in line with the results obtained with the linear classifier.

5. Discussion

Number agreement is a syntactic phenomenon that crucially relies on a proper parse of the structure of a sentence. In all five languages we considered, number agreement is made explicit through a form of morphological inflection that links subject and verb by virtue of their syntactic relationship and their shared grammatical number. Given the similarity of the underlying grammatical process, a truly multilingual neural model should display some degree of cross-lingual consistency in the neural units computing agreement. Our analyses showed that indeed there is a correspondence in the encoding of agreement patterns across languages, not only in terms of the layer-wise convergence of information, but also in terms of the organization of the neural units within a single layer. In the layer-wise analyses, a linear classifier built upon both mBERT and XLM-R embeddings was able to detect syntactic anomalies from the intermediate layers of the network. The classification accuracy decreased in the deepest layers of the networks, in line with results obtained with monolingual models (Jawahar, Sagot, and Seddah 2019); crucially, this quadratic concave trend was coherent across the languages included in our study. The structural alignment of different language pairs was susceptible to systematic differences affecting in particular Hebrew, a low-resource language that also obtains lower performance scores in layer-wise classification. We speculate that this difference in results might be due, at least in part, to the typological relations between the languages included in our study. Indeed, English, German, French, and Russian are Indo-European languages. Hebrew, on the other hand, is a Semitic language belonging to the Afroasiatic family,[7] despite exhibiting some Indo-European influences (Zuckermann 2006). Furthermore, differently from the others, Hebrew is a language characterized by a templatic morphology: Verbs and nouns can be inflected by modifying a consonantal root, adding vowels between the consonants. Hence, a linear segmentation of the input into sub-word units (as the one underlying mBERT and XLM-R tokenizers) might not capture the full morphological complexity of the words (Klein and Tsarfaty 2020). This entails that two inflected forms of the same root might not share any sub-word token more frequently than in languages with concatenative

7 Following the Omniglot classification of languages at `https://omniglot.com/writing/langfam.htm`.

morphological systems, making agreement computations more difficult and based on representational properties that are different from the other considered languages. We thus speculate that the weaker correspondence in the neural unit processing agreement in Hebrew might be motivated by these typological and morphological differences.

Despite a certain degree of language specificity in the intersection patterns, the independent selection of language-specific relevant units can nonetheless identify a shared substrate underlying number agreement processing. Across model types and ranking methods, the size of this shared substrate is consistently larger with increased distance between the two hierarchically dependent words, as evidenced by the higher *FE* in the long-distance condition. The greater distance between subject and verb, as well as the contingent introduction of attractors between them, makes the task of word prediction more difficult, as evidenced by standard predictive tests (Mueller et al. 2020). Hence, the comparison between the results obtained in the two agreement conditions suggests that cross-lingual alignment is favored by more complex sentence representations. A possible objection to this observation lies in the fact that both the training and the test set in the long-distance condition comprised more items than in the short-distance condition (see Section 3.3). This asymmetry in training data might have resulted in a more precise ranking in the long-distance case, which in turn could have identified more efficiently the cross-lingual components in the network. To rule out this possible confound, we repeated all our analyses after downsampling the long-distance set,[8] and still found a more consistent unit-level convergence with increased distance between the two interdependent constituents (see Appendix 3). Another factor that influenced the cross-lingual convergence of syntactic information was model type: The intersection sizes derived from the XLM-R-based ranks were much larger than the ones obtained from its predecessor, regardless of the neuron ranking algorithm (in line with previous results on probing with MMMs, see Antverg and Belinkov [2021] and Stanczak et al. [2022] for similar results). The two models are minimally different: The main attributes that distinguish them are the larger amount of training data and the absence of the NSP objective in XLM-R. This suggests that the NSP loss is not a crucial determinant of cross-lingual convergence, and that more trained and better performing multilingual models have stronger language-neutral internal components (see also Del and Fishel 2021).

From a methodological standpoint, the qualitative convergence in the results obtained with LCA and the probeless ranking method shows that our findings are not biased by the inherent limitations of the probing framework, such as the conflation between the information learned by the model and by the probe (Antverg and Belinkov 2021). Indeed, the main outcomes of our study—such as the greater cross-lingual convergence in long- versus short-distance agreement and the stronger alignment in the RoBERTa-based encoder—are robust regardless of the neuron ranking method applied.

6. Follow-up: The Depth of the Cross-lingual Syntax

In the previous sections, we started from the implicit assumption that the most relevant layers for computing agreement *within* a single language would show the highest consistency in their inner organization *across* languages. In the present follow-up study, we

8 We chose to rule out this confound a posteriori instead of performing our analyses on balanced sets from the beginning in order to derive more precise estimates for the log-distance condition, where more data were available.

empirically tested this premise. First, we examined the weights assigned by the linear classifiers to the highest scoring individual neurons across layers, and their dispersion across languages (6.1). Then, as a control, we also analyzed the layer-wise correlations between the weight matrices learned by the classifiers in the five different languages[9] (6.2).

6.1 Top Neurons Across Layers

Whereas in our previous experiments we adopted a maximally conservative approach by extracting five language-specific independent neuron rankings for each condition, here we used a more exploratory procedure by jointly searching for relevant cross-lingual neurons in each layer. We reasoned that a cross-lingual neuron responding to agreement should satisfy two necessary conditions. First, it should have, on average, a high impact on the prediction of the grammaticality label. Second, the measures of that neuron's impact in the five languages considered should be comparable: Its relevance should not be driven by a subset of the languages, but rather be cross-linguistically stable. Following this line of reasoning, we operationalized the cross-lingual relevance of each unit with respect to the task by averaging the absolute value of its weights learned by the five language-specific classifiers. This procedure allowed us to construct a global, language-neutral ranking of the neurons. Then, for each layer, we considered the neural unit with the highest average weight, and observed the relative standard deviation of its value across languages. We performed our analyses independently for short- and long-distance agreement, and for either model type.

The results of our follow-up tests are depicted in Figure 5. The general pattern that clearly emerges from the four plots is an initial increase in average weight, which is steeper in the long-distance condition; the average weights then decrease in the last layers. The growth in the average weight is associated with a contingent reduction in the cross-lingual measure of dispersion, as indicated by the error bars. In the case of mBERT, this rise in the average weight reaches its peak in the intermediate $[\![8, 9]\!]$ layers. In the short-distance condition, the highest weight is obtained in the eighth layer by neuron 6533 (5a); this neuron's weights also exhibit a contained amount of variation across languages (although the top neurons in the embedding and in the seventh layer display an even smaller amount of dispersion). The best candidate cross-lingual neuron is easier to identify in the long-distance condition: Neuron 7674 in the ninth layer exhibits at the same time the two preconditions identified above, being both the one with the highest weight and the one with the lowest cross-lingual deviation (5b). XLM-R neurons behave in an analogous way, but reach their maximal cross-lingual convergence in earlier layers. In the short-distance condition, the highest mean weight is obtained in the seventh layer by neuron 5621 (5c); this neuron also displays contained cross-lingual variation, although the weights of neuron 6545 in the eighth layer are more stable across languages. In the long distance condition, neuron 5066 in the sixth layer is the most relevant agreement-responding unit (5d); while neurons 5666, 6928, and 7931 are slightly more stable across languages, 5066 clearly marks the weight peak. In the case of XLM-R, the weight-by-layer growth curve is steeper if compared with mBERT, especially in the long-distance condition: While the weights of the top neurons in the first five layers are close to zero and highly variable across languages, from the sixth layer we have an almost sudden increment.

9 We thank the anonymous reviewers for the suggestion.

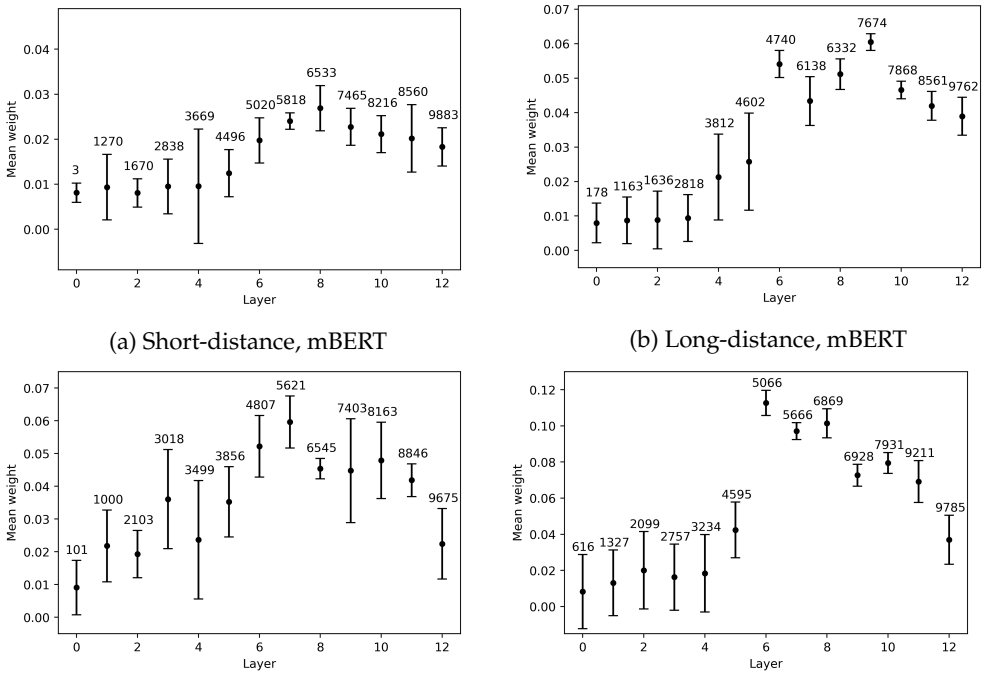

(a) Short-distance, mBERT

(b) Long-distance, mBERT

(c) Short-distance, XLM-R

(d) Long-distance, XLM-R

Figure 5
Mean weight of each layer's top neuron, averaged over five languages. The error bars indicate the relative standard variation of the weight across the five languages, rescaled by a 10^2 factor for readability purposes. The numbers annotated over the error bars specify the ID of the neuron whose metrics are depicted in the graph. Note that the y axis scale varies across plots, in order to highlight the layer-wise progression of the average weights.

6.2 Correlation Between Weight Matrices Across Layers

In the previous section, we considered the individual units of each layer that were assigned the highest average weight by the linear classifier, in order to draw conclusions about the layer-wise encoding of agreement across languages. This approach allowed us to identify a set of individual units that are cross-lingually associated with number agreement; however, this procedure neglects the vast majority of the network's units. Hence, as a sanity check, we also analyzed the cross-lingual correlation between the weights assigned by the linear classifiers to the neurons of each layer. The weights of the classifier are supposed to reflect the relevance of each unit with respect to the linguistic property being investigated, namely, grammatical agreement. Thus, a cross-lingual correlation in the classifier weights reflects how similarly two given languages encode agreement relations. Differently from our previous results, this analysis considers all the neural units within a layer, and not only the top neurons. Following our previous results, we predicted an increase in cross-lingual weight correlation in the first layers of the networks, followed by a plateau in the intermediate layers, and a final decrease toward the deepest layers of the models.

The layer-wise results of our weight correlation analysis are reported in Figure 6; note that each point in the plot reflects the average weight correlation obtained across

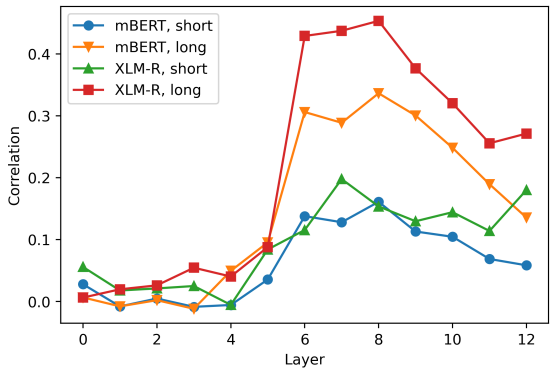

Figure 6
Layer-wise progression of cross-lingual weight correlations, grouped by model and condition.

the ten combinations of language pairs. All the pairwise correlations are reported in detail in Appendix 4 (Figure 10). The results of the correlation analyses are largely consistent with what we reported in the previous section. Across model types and conditions, the cross-lingual correlation in the weight matrices (henceforth CCWM) increases in the intermediate layers of the models, reaching its peak in the seventh (XLM-R, short-distance agreement) and eighth layer (mBERT, short- and long-distance agreement; XLM-R, long-distance agreement). Then, the CCWM progressively decreases toward the deepest layers of the models. While the localization of the correlation peaks does not coincide exactly with the weight maxima identified in § 6.1, from a qualitative standpoint the layer-wise progression of the CCWM is mostly coherent with our previous observations, when considering the effects of both agreement condition and model type. Indeed, the increase in CCWM is steeper (a) when considering long- as opposed to short-distance dependencies, and (b) when analyzing XLM-R as opposed to mBERT embeddings.

Taken together, these layer-wise patterns strengthen our previous findings in two ways. First, they confirm the premise of our first experiment concerning the layer-wise flow of cross-lingual syntactic information within the network, supporting our choice to constrain our tests to the middle layers of the network. Second, they clearly show that there is a cross-lingual convergence in the encoding of grammatical structures in the middle-to-deep layers of the networks. This means that MMMs such as mBERT and XLM-R progressively develop a cross-lingual space where language-neutral individual units respond to similar grammatical structures in different languages. Overall, these results are consistent with the view that identifies the first layers of an MMM as a multilingual encoder (Del and Fishel 2021), where syntactic features are progressively elaborated and converge toward the same units in the middle-to-deep layers. Then, the subsequent decline is coherent with the view of MMMs as the stacking of two subnetworks: a multilingual encoder followed by a task-specific decoder, which has little importance in the transfer (Muller et al. 2021).

6.3 Single Neurons Encode Grammatical Structures

In § 6.1, we identified four candidate cross-lingual neurons. These units were assigned on average a high weight by the linear classifier, and their relevance was characterized

by a reduced variation across languages. In this section, we studied their individual behavior in response to well-formed and agreement-violating sentences. More precisely, we tested whether their activation patterns alone were *sufficient* and *necessary* to predict the grammaticality of such sentences. To do so, we assessed whether (a) the activations of those units *alone* could predict agreement violations, and (b) the activations of their respective layers could predict grammaticality when these units were zeroed out. To increase the generalizability of our results, we measured their responses to agreement in another condition of the CLAMS dataset, across a Prepositional Phrase (e.g., "The surgeons behind the architect *smiles/smile"). This condition was chosen as it falls between the long-distance VP coordination and the short-distance condition in terms of the distance between subject and verb. A total of 11,200 sentences from this condition[10] were selected and divided in a train and a test set (80% train, 20% test). Then, we extracted the activations of the models in the verb position, and (a) selected the output of the four units identified in the previous section (neurons 7674 and 6533 in the case of mBERT, and neurons 5066 and 5621 for XLM-R), or (b) zeroed out their activations in the layers output. In the former case (a), we used the output of each of these neurons taken singularly as a predictor in a logistic regression model, with the dummy-coded label of grammatical acceptability as dependent variable. We then computed the classification accuracy in the test set, and assessed the statistical significance of our results against chance level with a binomial test. As an additional baseline, we also randomly sampled 30 neural units from the corresponding layers in the two models (layers 8 and 9 for mBERT, and 7 and 6 for XLM-R), and evaluated their average accuracy in predicting the grammaticality label on the same dataset.[11] In the second case (b), we used as predictors in the logistic regression models all the layer units except for the neuron of interest; we then compared the results obtained with the full layer embedding with the results obtained with the ablated layer by means of a McNemar test, a statistical test utilized on paired nominal data.

6.3.1 Single Neurons Are Sufficient to Compute Agreement. The results of our experiment are reported in Figure 7. Overall, the neurons that we identified in the previous section were significantly predictive of grammaticality across languages, providing a sanity check for our procedure. In the case of mBERT, the activation of neuron 7674, which had been singled out in the long-distance condition, was sufficient to significantly classify sentences as agreement-violating in all the languages considered, with an average accuracy of 0.59 (7a). Not surprisingly, accuracy was lower in the Russian and Hebrew datasets, but nonetheless the performance levels were still above chance. The activation of neuron 6533 achieved a rather inferior performance, as it reached statistical significance only in German and French, with an average cross-lingual accuracy of 0.53. As in all the tests we reported so far, the results obtained with XLM-R were more solid, as both neuron 5066 and 5621 were significant predictors of grammaticality in all languages (7b), with the exception of neuron 5621 in French, which was only marginally significant ($p = 0.056$). The logistic classifier based on neuron 5066 achieved an average accuracy of 0.64; notably, its output alone was sufficient to reach an accuracy level of 0.84 in French. Similarly to mBERT, the neuron identified in the short-distance condition (5621) was less strongly associated with the label in most languages, but it still obtained

10 The number of instances was chosen to match the smallest challenge set (in Hebrew) for cross-lingual comparability.

11 We thank an anonymous reviewer for the suggestion.

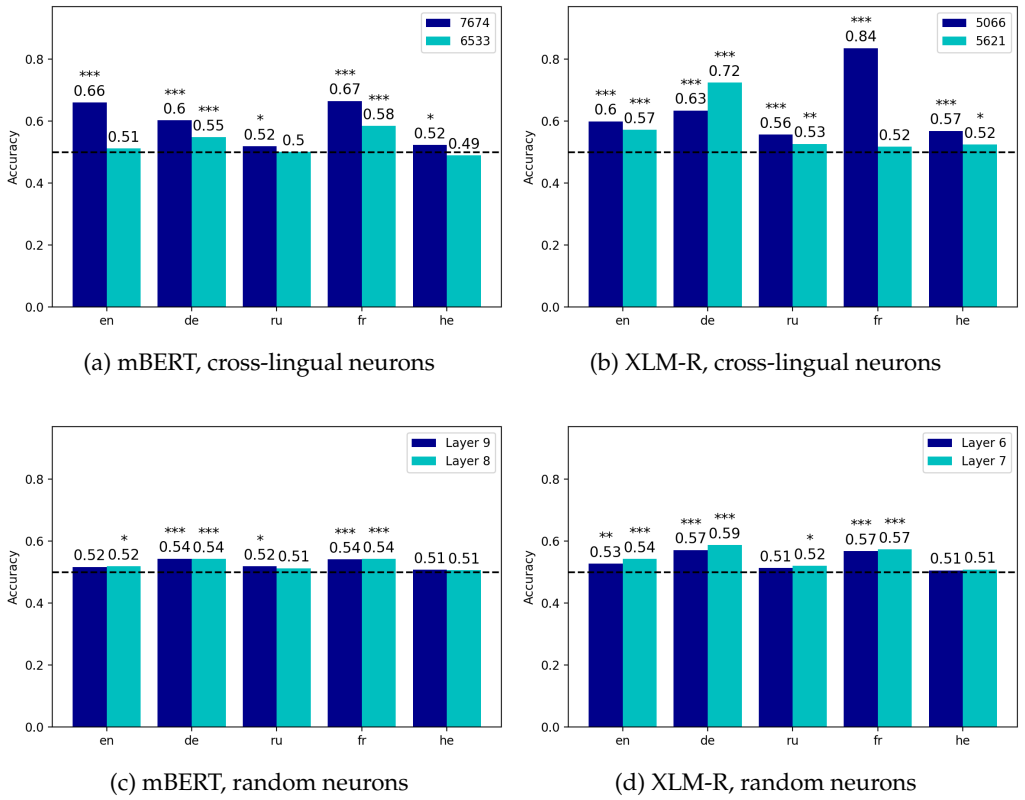

(a) mBERT, cross-lingual neurons

(b) XLM-R, cross-lingual neurons

(c) mBERT, random neurons

(d) XLM-R, random neurons

Figure 7
Accuracy of the classifiers based on the neurons identified in Section 6 (top row) and average performance obtained by 30 units randomly sampled from the same layer (bottom row), grouped by language. The asterisks indicate the statistical significance of the results against chance level, with $p < 0.001$***, $p < 0.01$**, $p < 0.05$*.

an average accuracy of 0.57. If compared to randomly sampled units from the same layers, which in theory could be expected to respond to similar linguistic phenomena, the neurons extracted with our procedure were generally more effective in predicting the well-formedness of a sentence. Across both model types, the neurons identified in the long-distance condition (7674 and 5066) consistently outperformed in classification accuracy the randomly sampled units extracted from their respective layers, with the only exception the Russian data, where the outcomes were comparable. Once again, the results in the short-distance condition are less clear-cut. In the case of mBERT, neuron 6533 outperformed the randomly sampled baseline only in German and French, but when considering the RoBERTa-based transformer, neuron 5621 outperformed the baseline in all the languages but French. However, it should be noted that the neurons that we randomly sampled from the relevant layers generally obtained above-chance performance scores in the classification task, suggesting that number agreement computations are spread out across the middle layers of the network.

6.3.2 Single Neurons Are not Necessary to Compute Agreement. Once verified that the four interlingual neurons we singled out in § 6.1 were *sufficient* to capture agreement

Table 1
Comparison of the results of the classifier obtained with the full layer and the ablated layer. The first two columns indicate the language and the agreement condition where the units were identified (see § 6.1). The following five columns specify the results obtained with mBERT, and in particular the target neuron that was zeroed out, the respective layer, the accuracy obtained with the full layer embedding, the accuracy obtained with the ablated layer, and the statistical significance of the McNemar test. The last five columns report the same indexes, but relative to the XLM-R model. *In contrasting the accuracy of the full and the ablated layer, the standard χ^2 calculation was used instead of the binomial test, as the number of observations per cell in the contingency table was higher than 25.

		mBERT					XLM-R				
Language	Cond.	Neuron	L	Acc	Acc_{abl}	p	Neuron	L	Acc	Acc_{abl}	p
French	Short	6533	8	1.0000	1.0000	1.0000	5621	7	1.0000	1.0000	1.0000
French	Long	7674	9	1.0000	1.0000	1.0000	5066	6	1.0000	1.0000	1.0000
English	Short	6533	8	0.9464	0.9451	0.2500	5621	7	0.9527	0.9527	1.0000
English	Long	7674	9	0.9549	0.9558	0.6250	5066	6	0.9049	0.9040	0.7540
Hebrew	Short	6533	8	0.9013	0.9013	1.0000	5621	7	0.8710	0.8705	1.0000*
Hebrew	Long	7674	9	0.8933	0.8942	0.6880	5066	6	0.8299	0.8326	0.4170
Russian	Short	6533	8	0.9821	0.9821	1.0000	5621	7	0.9254	0.9259	1.0000
Russian	Long	7674	9	0.9754	0.9754	1.0000	5066	6	0.8777	0.8790	0.6640
German	Short	6533	8	1.0000	1.0000	1.0000	5621	7	1.0000	1.0000	1.0000
German	Long	7674	9	1.0000	1.0000	1.0000	5066	6	1.0000	1.0000	1.0000

violations with an above-chance performance, we aimed to test whether their contribution was *necessary* for the task. The results of these analyses are summarized in Table 1. As can be seen in the table, the ablation of the candidate cross-lingual units did not show a significant impact on the results obtained by the classifiers in any of the languages considered in the analyses, regardless of model type. This result is largely consistent with our previous observation that number agreement processing is not restricted to a small number of specialized units in multilingual transformer models, but it is encoded with redundancy in the network's embeddings. While the activation patterns of the neurons we set apart in our cross-lingual search do encode agreement to a significant extent, their role is not decisive in agreement processing.

6.4 Testing in an Unseen Language

In the previous section, we tested the four candidate interlingual neurons we identified in § 6.1 in a novel condition of the CLAMS dataset, showing that our selection procedure was robust to small changes in the sentential structure of the agreement data. To further assess the cross-lingual abilities of those units, we further extended the analyses to measure their predictive power in detecting agreement violations in an *unseen language*, that is, Italian. Since the CLAMS dataset did not include any other language beyond the ones that we had previously considered, we artificially created a new agreement dataset in a rule-based fashion, and replicated our previous analyses in this dataset.

6.4.1 Dataset Creation and Analyses. To generate an agreement dataset in Italian, we started from a set of 2 determiners (definite and indefinite; D), 20 nouns (N), 20 verbs (10 transitive, 10 intransitive; V), and 15 temporal prepositional modifiers (M). Then, we created a corresponding plural set for each of D, N, and V (D_p, N_p, V_p). Starting

from those samples, we created four agreement conditions by computing the Cartesian products between the three sets:[12]

(a) Singular agreement: $D \times N \times V$

(b) Plural agreement: $D_p \times N_p \times V_p$

(c) Violated singular agreement: $D \times N \times V_p$

(d) Violated plural agreement: $D_p \times N_p \times V$

where each condition consisted of 800 items. We then inserted one modifier sampled from *M* after the nouns, to increase the distance between subject and verb to an amount comparable to the CLAMS condition we used in § 6.3 (across a Prepositional Phrase). Conditions (a) and (b) were then merged and labeled as grammatical, whereas conditions (c) and (d) were codified as ungrammatical. This method allowed us to generate 3,200 labeled sentences, which were then divided in a train (80%) and a test set (20%). Following our previous procedures, we used the two transformer models to extract their internal activations in the verb position; then, we selected from the obtained embeddings the output of the four candidate cross-lingual units (mBERT: 6533, 7674; XLM-R: 5621, 5066). We then trained four different logistic regression models—one for the output of each neuron—in the training set data, and evaluated their accuracy in the test set. Beside contrasting the model accuracy against chance level with a binomial test, we implemented a second baseline with 30 neural units randomly sampled from the same layers as the target neurons.

6.4.2 Results. The neural units that we consider in this study were generally successful in detecting agreement violations in Italian. When considering mBERT, the neuron identified in the short-distance condition (6533) reached an accuracy score of 0.57 (p = 0.0001); the unit that had been singled out in the long-distance condition (7674) obtained an accuracy of 0.52, although the binomial test was not significant (p = 0.1258). On the other hand, both the units that were identified in the XLM-R model significantly outperformed chance level (5621: 0.60, $p = 1.56 \cdot 10^{-7}$; 5066: 0.64, $p = 1.63 \cdot 10^{-13}$). The randomly sampled units obtained instead a rather inferior performance in the Italian test set, with the exception of the sample based on the ninth layer of mBERT (mBERT, layer 8: 0.53, p = 0.0525; mBERT, layer 9: 0.53, p = 0.0446; XLM-R, layer 7: 0.54, p = 0.0219; XLM-R, layer 6: 0.51, p = 0.3319). Taken together, these results strengthen the validity of our methodology, showing that the neural units that were associated with agreement in a set of languages can successfully capture the same property in a different language which did not concur in the unit selection.

The performance of individual neurons in predicting well-formedness demonstrates that explicit knowledge emerges in a quasi-symbolic format in the neural units we identified in the previous experiment. Interestingly, simply training a transformer model on a masked language modeling objective on multilingual data causes the emergence of syntax-sensitive units that respond to the same linguistic phenomenon in different languages. The knowledge encoded in these units is also sufficiently abstracted

12 Note that the agreement relationship between *D* and *N* was set to always be grammatical, so that the only structure-dependent relationship that could be violated was subject-verb number agreement.

from the low-level features of the input that can be captured even in settings that differ from the one employed during unit selection, both in terms of agreement conditions (across a Prepositional Phrase) and languages (Italian). However, the comparison with randomly sampled neurons further shows that while some units are particularly responsive to agreement violations, this grammatical phenomenon is encoded with redundancy in the network's embeddings. Indeed, other randomly sampled dimensions in the activation matrix still respond to the same structure-dependent relationship, although with lower levels of association with the label (see Dalvi et al. [2020] for an analysis of redundancy in transformer language models). This finding is congruent with the layer ablation results, where we showed that the activation patterns of the target neurons were not necessary to reach near-perfect accuracy in the classification task.

7. Conclusion

This study presents the first single-neuron analysis aimed at assessing the cross-lingual nature of mBERT and XLM-R agreement processing mechanisms. Our findings are in line with the view that the very large neural capacity in MMMs leads to multilingual representations that have both language-neutral and language-specific components (see also Doddapaneni et al. 2021; Gonen, Ravfogel, and Goldberg 2022). While the majority of the networks' units shows a heterogeneous cross-lingual relevance, several neurons in the structural embeddings of mBERT and XLM-R respond to syntactic features in two or more languages. We argue that those neurons can be considered as the implementational substrate that supports number agreement computations across languages. The independent neuron rankings, while far from being identical, display an above-chance level of cross-lingual consistency. This consistency is stronger for long- vis-à-vis short-distance agreement, suggesting that more complex structures tax more strongly the language-neutral components of the networks. Our results are also informative in terms of model comparison: While most research efforts considered a single model—generally mBERT—when assessing the eventual cross-lingual nature of its representations (Singh et al. 2019; Chi, Hewitt, and Manning 2020; Dufter and Schütze 2020; Muller et al. 2021; Guarasci et al. 2022, although see Del and Fishel 2021), our results contrast two prominent MMMs, showing that the RoBERTa-based transformer excels in cross-lingual alignment. With respect to the previous literature, our study is novel in that it measures the convergence of cross-lingual signal in the syntactic domain. Previous studies often used a coarse-grained approach to cross-lingual coherence; indeed, the emergence of an interlingual space was often measured as the layer-wise progression of sentence similarity scores across languages, thus conflating syntactic and semantic features (e.g., Singh et al. 2019; Del and Fishel 2021; but see Chi, Hewitt, and Manning 2020). In this study, we extended the previous findings by showing that even when narrowing the scope of our analyses to subtle structure-dependent phenomena, the models consistently allocate an overlapping set of resources to similar processes across languages. In the Introduction, we mentioned how the study of the convergence of information in a multilingual neural model could inform the debate on the neural underpinnings of linguistic knowledge in multilingual individuals. In that respect, our study shows that the optimal solution that naturally emerges from priorless sequence processing networks is a partial overlap of resources, which is dependent on the typological similarity between languages.

The very existence of language-neutral components in mBERT and XLM-R shows that the models address the high surface inconsistency of the multilingual input through

strong generalization—hence, leveraging truly multilingual knowledge. Once acknowledged that the representation space exploited by MMMs is multilingual in nature, the study of their predictive behavior could provide us with unique insights into the structural symmetries that are instantiated across languages, and inform us on the nature of language as a system beyond the surface discrepancies shown by single languages. We hope that this investigation will pave the way to future studies inspecting the MMMs' learned representation spaces to acquire novel knowledge on the properties that are shared across languages and language families.

8. Limitations and Further Directions

This study showed that number agreement is partly encoded by a language-neutral set of parameters in the structural embeddings of mBERT and XLM-R. However, two important caveats must be made. First, the syntactic relationship we analyze is a circumscribed expression of the variety of grammatical phenomena that characterize natural languages. While restricting our analyses to a specific class of grammatical instances increases the experimental control over our study, it should be noted that the generalizability of our findings to other linguistic structures should be properly assessed in future research. Second, the phenomenon we investigate is expressed in our language sample in a rather consistent way, when analyzed in abstract terms: Subject and verb are paired through a form of morphological inflection—which is mainly concatenative in four out of the five languages considered—on account of their structural dependency and their grammatical number. We leave for future research an assessment of whether our results hold when considering a more typologically diverse language sample that conveys agreements relationships in fundamentally different ways.

Appendix 1. Weight Mass Analyses

In § 4, we considered the number of top 100 units that were shared among two or more languages to draw conclusions on the neuron-level cross-lingual convergence of agreement information in the networks. However, the threshold we used, while congruent with previous research (Antverg and Belinkov 2021), needs to be motivated. In particular, it is necessary to ensure that the top neurons that are considered in the analyses effectively account for a sufficiently ample proportion of the weight mass. In other words, it is critical to verify that (a) the weight distribution is sufficiently skewed to motivate the selection of N top neurons, and (b) N = 100 is a sensible threshold that includes the most relevant units, and does not include too many of the non-relevant ones. To verify these premises, we plot the weight distribution of the different model × condition × language combinations, and examine the ratio of the cumulative weight mass[13] accounted for by the top 100 units. The outcomes of these analyses are summarized in Figure 8. As can be clearly seen from the figure, the weight distributions are highly skewed, with a small number of units that are assigned high weights, and a long right tail of less relevant neurons. In general, 100 neurons—which only constitute 13.02% of the layer units—contribute to a substantial proportion of the weight mass of the layer (on average 45.46%). This proportion is lower when considering mBERT

13 $\frac{\sum_{i=1}^{100} w_i}{\sum_{j=1}^{768} w_j}$

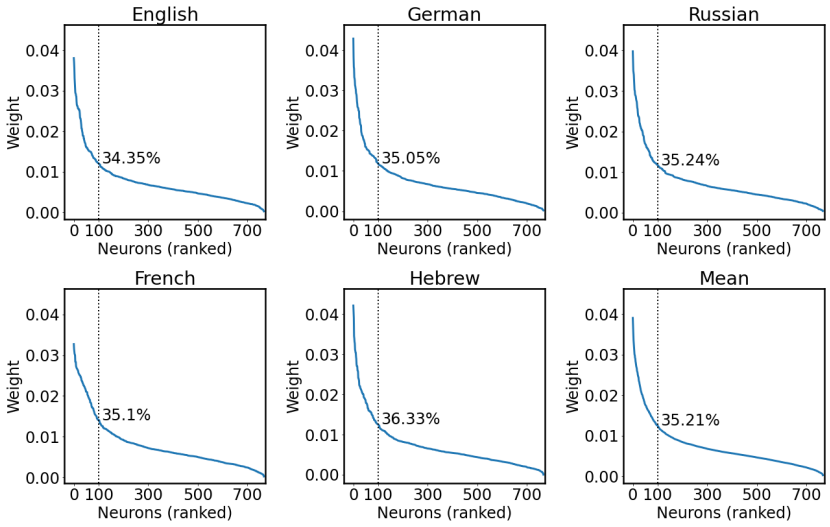

(a) Short-distance, mBERT, layer 8

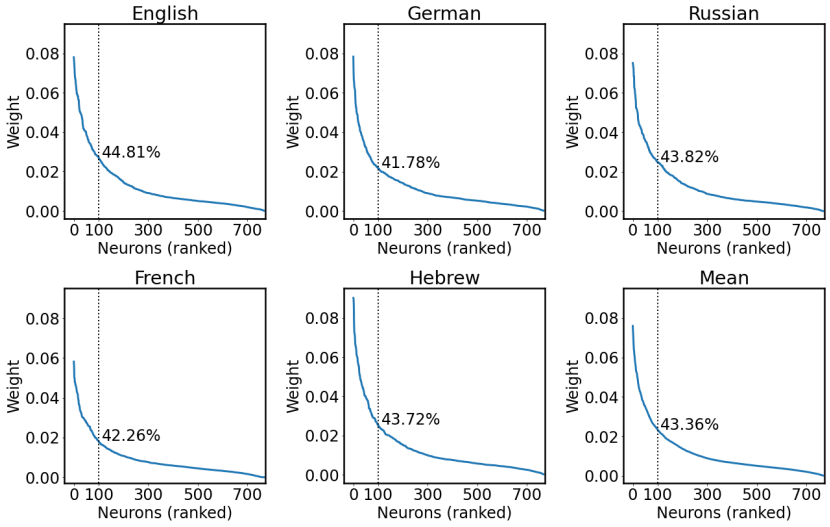

(b) Long-distance, mBERT, layer 9

Figure 8
Weights (y axis) associated by the linear classifier to the individual units (x axis) of the relevant layers. The percentage superimposed on the graph indicates the cumulative weight mass accounted for by the top 100 units in each individual language.

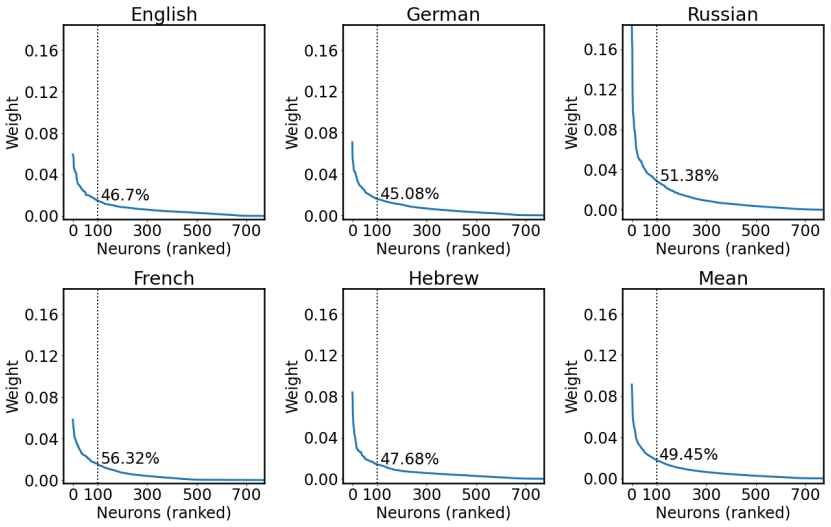

(c) Short-distance, XLM-R, layer 7

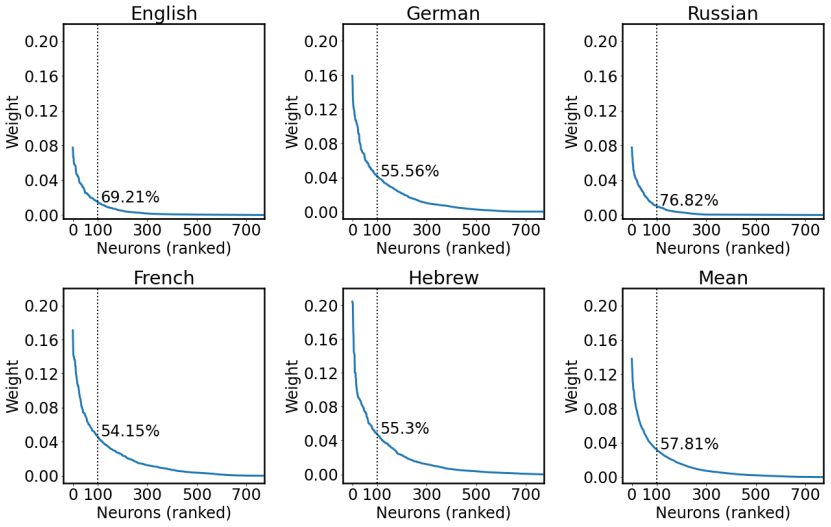

(d) Long-distance, XLM-R, layer 7

(short-distance: 35.21%; long-distance: 43.36%) as opposed to XLM-R (short-distance: 49.45%; long-distance: 57.81), and with short- as opposed to long-distance dependencies between subject and verb (see above). This suggests that both model type and subject-verb distance contribute to the sparseness of the encoding of the phenomenon under scrutiny, with XLM-R and long-distance dependencies causing the emergence of fewer specialized units that respond to agreement violations, and mBERT and short-distance agreement promoting more distributed and possibly redundant encoding patterns. However, despite a certain amount of variability across models and conditions, 100 units generally contribute to a large amount of the weight mass, justifying a posteriori the choice of our threshold.

Appendix 2. Super Exact Test Results in Detail

2.1. Linguistic Correlation Analysis

Table 2
Results of the super exact test relative to all $N_{2\ldots5}$-way intersections of the top 100 neurons in the short-distance agreement condition (mBERT, LCA).

Intersection	Degree	Obs. overlap	Exp. overlap	*FE*	*p*
Fr ∩ Ru	2	28	13.0208	2.1504	$1.21 \cdot 10^{-05}$
He ∩ Ru	2	26	13.0208	1.9968	$1.17 \cdot 10^{-04}$
He ∩ Fr	2	19	13.0208	1.4592	$4.47 \cdot 10^{-02}$
En ∩ Ru	2	25	13.0208	1.9200	$3.34 \cdot 10^{-04}$
En ∩ Fr	2	39	13.0208	2.9952	$5.84 \cdot 10^{-13}$
En ∩ He	2	14	13.0208	1.0752	$4.28 \cdot 10^{-01}$
De ∩ Ru	2	17	13.0208	1.3056	$1.34 \cdot 10^{-01}$
De ∩ Fr	2	34	13.0208	2.6112	$3.03 \cdot 10^{-09}$
De ∩ He	2	15	13.0208	1.1520	$3.10 \cdot 10^{-01}$
De ∩ En	2	29	13.0208	2.2272	$3.54 \cdot 10^{-06}$
He ∩ Fr ∩ Ru	3	8	1.6954	4.7186	$2.29 \cdot 10^{-04}$
En ∩ Fr ∩ Ru	3	10	1.6954	5.8982	$4.68 \cdot 10^{-06}$
En ∩ He ∩ Ru	3	6	1.6954	3.5389	$6.33 \cdot 10^{-03}$
En ∩ He ∩ Fr	3	9	1.6954	5.3084	$3.50 \cdot 10^{-05}$
De ∩ Fr ∩ Ru	3	10	1.6954	5.8982	$4.68 \cdot 10^{-06}$
De ∩ He ∩ Ru	3	5	1.6954	2.9491	$2.59 \cdot 10^{-02}$
De ∩ He ∩ Fr	3	7	1.6954	4.1288	$1.30 \cdot 10^{-03}$
De ∩ En ∩ Ru	3	6	1.6954	3.5389	$6.33 \cdot 10^{-03}$
De ∩ En ∩ Fr	3	17	1.6954	10.027	$1.58 \cdot 10^{-13}$
De ∩ En ∩ He	3	5	1.6954	2.9491	$2.59 \cdot 10^{-02}$
En ∩ He ∩ Fr ∩ Ru	4	4	0.2208	18.1194	$6.82 \cdot 10^{-05}$
De ∩ He ∩ Fr ∩ Ru	4	3	0.2208	13.5895	$1.38 \cdot 10^{-03}$
De ∩ En ∩ Fr ∩ Ru	4	5	0.2208	22.6492	$2.59 \cdot 10^{-06}$
De ∩ En ∩ He ∩ Ru	4	3	0.2208	13.5895	$1.38 \cdot 10^{-03}$
De ∩ En ∩ He ∩ Fr	4	5	0.2208	22.6492	$2.59 \cdot 10^{-06}$
De ∩ En ∩ He ∩ Fr ∩ Ru	5	3	0.0287	104.3677	$3.39 \cdot 10^{-06}$

Table 3
Long-distance agreement condition (mBERT, LCA).

Intersection	Degree	Obs. overlap	Exp. overlap	*FE*	*p*
Fr ∩ Ru	2	40	13.0208	3.0720	$8.85 \cdot 10^{-14}$
He ∩ Ru	2	24	13.0208	1.8432	$8.90 \cdot 10^{-04}$
He ∩ Fr	2	18	13.0208	1.3824	$8.03 \cdot 10^{-02}$
En ∩ Ru	2	26	13.0208	1.9968	$1.17 \cdot 10^{-04}$
En ∩ Fr	2	38	13.0208	2.9184	$3.64 \cdot 10^{-12}$
En ∩ He	2	21	13.0208	1.6128	$1.13 \cdot 10^{-02}$
De ∩ Ru	2	35	13.0208	2.6880	$6.17 \cdot 10^{-10}$
De ∩ Fr	2	27	13.0208	2.0736	$3.90 \cdot 10^{-05}$
De ∩ He	2	24	13.0208	1.8432	$8.90 \cdot 10^{-04}$
De ∩ En	2	31	13.0208	2.3808	$2.51 \cdot 10^{-07}$
He ∩ Fr ∩ Ru	3	9	1.6954	5.3084	$3.50 \cdot 10^{-05}$
En ∩ Fr ∩ Ru	3	16	1.6954	9.4372	$2.50 \cdot 10^{-12}$
En ∩ He ∩ Ru	3	8	1.6954	4.7186	$2.29 \cdot 10^{-04}$
En ∩ He ∩ Fr	3	10	1.6954	5.8982	$4.68 \cdot 10^{-06}$
De ∩ Fr ∩ Ru	3	16	1.6954	9.4372	$2.50 \cdot 10^{-12}$
De ∩ He ∩ Ru	3	12	1.6954	7.0779	$5.83 \cdot 10^{-08}$
De ∩ He ∩ Fr	3	9	1.6954	5.3084	$3.50 \cdot 10^{-05}$
De ∩ En ∩ Ru	3	15	1.6954	8.8474	$3.59 \cdot 10^{-11}$
De ∩ En ∩ Fr	3	17	1.6954	10.0270	$1.58 \cdot 10^{-13}$
De ∩ En ∩ He	3	11	1.6954	6.4881	$5.54 \cdot 10^{-07}$
En ∩ He ∩ Fr ∩ Ru	4	6	0.2208	27.1791	$7.95 \cdot 10^{-08}$
De ∩ He ∩ Fr ∩ Ru	4	6	0.2208	27.1791	$7.95 \cdot 10^{-08}$
De ∩ En ∩ Fr ∩ Ru	4	10	0.2208	45.2985	$1.22 \cdot 10^{-14}$
De ∩ En ∩ He ∩ Ru	4	6	0.2208	27.1791	$7.95 \cdot 10^{-08}$
De ∩ En ∩ He ∩ Fr	4	7	0.2208	31.7089	$2.00 \cdot 10^{-09}$
De ∩ En ∩ He ∩ Fr ∩ Ru	5	4	0.0287	139.1569	$2.12 \cdot 10^{-08}$

Table 4
Short-distance agreement condition (XLM-R, LCA).

Intersection	Degree	Obs. overlap	Exp. overlap	*FE*	*p*
Fr ∩ Ru	2	32	13.0208	2.4576	$6.13 \cdot 10^{-08}$
He ∩ Ru	2	30	13.0208	2.3040	$9.74 \cdot 10^{-07}$
He ∩ Fr	2	31	13.0208	2.3808	$2.52 \cdot 10^{-07}$
En ∩ Ru	2	32	13.0208	2.4576	$6.13 \cdot 10^{-08}$
En ∩ Fr	2	35	13.0208	2.6880	$6.17 \cdot 10^{-10}$
En ∩ He	2	25	13.0208	1.9200	$3.34 \cdot 10^{-04}$
De ∩ Ru	2	21	13.0208	1.6128	$1.14 \cdot 10^{-02}$
De ∩ Fr	2	23	13.0208	1.7664	$2.22 \cdot 10^{-03}$
De ∩ He	2	28	13.0208	2.1504	$1.21 \cdot 10^{-05}$
De ∩ En	2	29	13.0208	2.2272	$3.54 \cdot 10^{-06}$
He ∩ Fr ∩ Ru	3	16	1.6954	9.4372	$2.50 \cdot 10^{-12}$
En ∩ Fr ∩ Ru	3	14	1.6954	8.2575	$4.68 \cdot 10^{-10}$
En ∩ He ∩ Ru	3	13	1.6954	7.6677	$5.51 \cdot 10^{-09}$
En ∩ He ∩ Fr	3	14	1.6954	8.2575	$4.68 \cdot 10^{-10}$
De ∩ Fr ∩ Ru	3	9	1.6954	5.3084	$3.50 \cdot 10^{-05}$
De ∩ He ∩ Ru	3	12	1.6954	7.0778	$5.84 \cdot 10^{-08}$
De ∩ He ∩ Fr	3	13	1.6954	7.6677	$5.51 \cdot 10^{-09}$
De ∩ En ∩ Ru	3	12	1.6954	7.0779	$5.84 \cdot 10^{-08}$
De ∩ En ∩ Fr	3	14	1.6954	8.2575	$4.68 \cdot 10^{-10}$
De ∩ En ∩ He	3	15	1.6954	8.8474	$3.59 \cdot 10^{-11}$
En ∩ He ∩ Fr ∩ Ru	4	9	0.2208	40.7686	$7.79 \cdot 10^{-13}$
De ∩ He ∩ Fr ∩ Ru	4	7	0.2208	31.7089	$2.01 \cdot 10^{-09}$
De ∩ En ∩ Fr ∩ Ru	4	7	0.2208	31.7089	$2.01 \cdot 10^{-09}$
De ∩ En ∩ He ∩ Ru	4	9	0.2208	40.7686	$7.79 \cdot 10^{-13}$
De ∩ En ∩ He ∩ Fr	4	11	0.2208	49.8283	$1.69 \cdot 10^{-16}$
De ∩ En ∩ He ∩ Fr ∩ Ru	5	6	0.0287	208.7354	$3.87 \cdot 10^{-13}$

Table 5
Long-distance agreement condition (XLM-R, LCA).

Intersection	Degree	Obs. overlap	Exp. overlap	*FE*	*p*
Fr ∩ Ru	2	54	13.0208	4.1472	$5.84 \cdot 10^{-28}$
He ∩ Ru	2	34	13.0208	2.6112	$3.03 \cdot 10^{-09}$
He ∩ Fr	2	30	13.0208	3.3040	$9.74 \cdot 10^{-07}$
En ∩ Ru	2	48	13.0208	3.6864	$2.94 \cdot 10^{-21}$
En ∩ Fr	2	48	13.0208	3.6864	$2.94 \cdot 10^{-21}$
En ∩ He	2	18	13.0208	1.3824	$8.04 \cdot 10^{-02}$
De ∩ Ru	2	54	13.0208	4.1472	$5.84 \cdot 10^{-28}$
De ∩ Fr	2	57	13.0208	4.3776	$1.12 \cdot 10^{-31}$
De ∩ He	2	26	13.0208	1.9968	$1.18 \cdot 10^{-04}$
De ∩ En	2	52	13.0208	3.9936	$1.28 \cdot 10^{-25}$
He ∩ Fr ∩ Ru	3	22	1.6954	12.9761	$4.42 \cdot 10^{-20}$
En ∩ Fr ∩ Ru	3	36	1.6954	21.2337	$6.28 \cdot 10^{-43}$
En ∩ He ∩ Ru	3	13	1.6954	7.6677	$5.51 \cdot 10^{-09}$
En ∩ He ∩ Fr	3	15	1.6954	8.8474	$3.59 \cdot 10^{-11}$
De ∩ Fr ∩ Ru	3	42	1.6954	24.7726	$1.29 \cdot 10^{-54}$
De ∩ He ∩ Ru	3	19	1.6954	11.2067	$4.90 \cdot 10^{-16}$
De ∩ He ∩ Fr	3	21	1.6954	12.3863	$1.07 \cdot 10^{-18}$
De ∩ En ∩ Ru	3	38	1.6954	22.4133	$1.07 \cdot 10^{-46}$
De ∩ En ∩ Fr	3	35	1.6954	20.6438	$4.33 \cdot 10^{-41}$
De ∩ En ∩ He	3	13	1.6954	7.6677	$5.51 \cdot 10^{-09}$
En ∩ He ∩ Fr ∩ Ru	4	12	0.2208	54.3582	$2.04 \cdot 10^{-18}$
De ∩ He ∩ Fr ∩ Ru	4	17	0.2208	77.0074	$9.49 \cdot 10^{-29}$
De ∩ En ∩ Fr ∩ Ru	4	30	0.2208	135.8955	$1.52 \cdot 10^{-60}$
De ∩ En ∩ He ∩ Ru	4	11	0.2208	49.8283	$1.69 \cdot 10^{-16}$
De ∩ En ∩ He ∩ Fr	4	12	0.2208	54.3582	$2.04 \cdot 10^{-18}$
De ∩ En ∩ He ∩ Fr ∩ Ru	5	10	0.0287	347.8924	$1.29 \cdot 10^{-23}$

2.2. Probeless

Table 6
Short-distance agreement condition (mBERT, probeless).

Intersection	Degree	Obs. overlap	Exp. overlap	*FE*	*p*
Fr ∩ Ru	2	26	13.0208	1.9968	$1.18 \cdot 10^{-04}$
He ∩ Ru	2	30	13.0208	3.3040	$9.74 \cdot 10^{-07}$
He ∩ Fr	2	31	13.0208	2.3808	$2.52 \cdot 10^{-07}$
En ∩ Ru	2	21	13.0208	1.6128	$1.14 \cdot 10^{-02}$
En ∩ Fr	2	54	13.0208	4.1472	$5.84 \cdot 10^{-28}$
En ∩ He	2	18	13.0208	1.3824	$8.04 \cdot 10^{-02}$
De ∩ Ru	2	30	13.0208	3.3040	$9.74 \cdot 10^{-07}$
De ∩ Fr	2	50	13.0208	3.8400	$2.19 \cdot 10^{-23}$
De ∩ He	2	23	13.0208	1.7664	$2.22 \cdot 10^{-03}$
De ∩ En	2	48	13.0208	3.6864	$2.94 \cdot 10^{-21}$
He ∩ Fr ∩ Ru	3	11	1.6954	6.4881	$5.55 \cdot 10^{-07}$
En ∩ Fr ∩ Ru	3	13	1.6954	7.6677	$5.51 \cdot 10^{-09}$
En ∩ He ∩ Ru	3	9	1.6954	5.3084	$3.5 \cdot 10^{-05}$
En ∩ He ∩ Fr	3	15	1.6954	8.8474	$3.59 \cdot 10^{-11}$
De ∩ Fr ∩ Ru	3	16	1.6954	9.4372	$2.5 \cdot 10^{-12}$
De ∩ He ∩ Ru	3	14	1.6954	8.2575	$4.68 \cdot 10^{-10}$
De ∩ He ∩ Fr	3	13	1.6954	7.6677	$5.51 \cdot 10^{-09}$
De ∩ En ∩ Ru	3	10	1.6954	5.8982	$4.69 \cdot 10^{-06}$
De ∩ En ∩ Fr	3	35	1.6954	20.6438	$4.33 \cdot 10^{-41}$
De ∩ En ∩ He	3	11	1.6954	6.4881	$5.55 \cdot 10^{-07}$
En ∩ He ∩ Fr ∩ Ru	4	6	0.2208	27.1791	$7.95 \cdot 10^{-08}$
De ∩ He ∩ Fr ∩ Ru	4	7	0.2208	31.7089	$2.01 \cdot 10^{-09}$
De ∩ En ∩ Fr ∩ Ru	4	7	0.2208	31.7089	$2.01 \cdot 10^{-09}$
De ∩ En ∩ He ∩ Ru	4	6	0.2208	27.1791	$7.95 \cdot 10^{-08}$
De ∩ En ∩ He ∩ Fr	4	8	0.2208	36.2388	$4.28 \cdot 10^{-11}$
De ∩ En ∩ He ∩ Fr ∩ Ru	5	3	0.0287	104.3677	$3.39 \cdot 10^{-06}$

Table 7
Long-distance agreement condition (mBERT, probeless).

Intersection	Degree	Obs. overlap	Exp. overlap	*FE*	*p*
Fr ∩ Ru	2	60	13.0208	4.608	$1.21 \cdot 10^{-35}$
He ∩ Ru	2	42	13.0208	3.2256	$1.7 \cdot 10^{-15}$
He ∩ Fr	2	38	13.0208	2.9184	$3.64 \cdot 10^{-12}$
En ∩ Ru	2	37	13.0208	2.8416	$2.14 \cdot 10^{-11}$
En ∩ Fr	2	36	13.0208	2.7648	$1.18 \cdot 10^{-10}$
En ∩ He	2	26	13.0208	1.9968	$1.18 \cdot 10^{-04}$
De ∩ Ru	2	52	13.0208	3.9936	$1.28 \cdot 10^{-25}$
De ∩ Fr	2	57	13.0208	4.3776	$1.12 \cdot 10^{-31}$
De ∩ He	2	36	13.0208	2.7648	$1.18 \cdot 10^{-10}$
De ∩ En	2	45	13.0208	3.4560	$2.92 \cdot 10^{-18}$
He ∩ Fr ∩ Ru	3	30	1.6954	17.6947	$2.29 \cdot 10^{-32}$
En ∩ Fr ∩ Ru	3	27	1.6954	15.9253	$1.64 \cdot 10^{-27}$
En ∩ He ∩ Ru	3	17	1.6954	10.027	$1.59 \cdot 10^{-13}$
En ∩ He ∩ Fr	3	17	1.6954	10.027	$1.59 \cdot 10^{-13}$
De ∩ Fr ∩ Ru	3	39	1.6954	23.0031	$1.25 \cdot 10^{-48}$
De ∩ He ∩ Ru	3	26	1.6954	15.3354	$5.85 \cdot 10^{-26}$
De ∩ He ∩ Fr	3	24	1.6954	14.1558	$5.94 \cdot 10^{-23}$
De ∩ En ∩ Ru	3	26	1.6954	15.3354	$5.85 \cdot 10^{-26}$
De ∩ En ∩ Fr	3	29	1.6954	17.1049	$1.02 \cdot 10^{-30}$
De ∩ En ∩ He	3	17	1.6954	10.027	$1.59 \cdot 10^{-13}$
En ∩ He ∩ Fr ∩ Ru	4	13	0.2208	58.888	$2.19 \cdot 10^{-20}$
De ∩ He ∩ Fr ∩ Ru	4	18	0.2208	81.5373	$5.93 \cdot 10^{-31}$
De ∩ En ∩ Fr ∩ Ru	4	22	0.2208	99.6567	$3.45 \cdot 10^{-40}$
De ∩ En ∩ He ∩ Ru	4	13	0.2208	58.888	$2.19 \cdot 10^{-20}$
De ∩ En ∩ He ∩ Fr	4	14	0.2208	63.4179	$2.09 \cdot 10^{-22}$
De ∩ En ∩ He ∩ Fr ∩ Ru	5	10	0.0287	347.8924	$1.29 \cdot 10^{-23}$

Table 8
Short-distance agreement condition (XLM-R, probeless).

Intersection	Degree	Obs. overlap	Exp. overlap	*FE*	*p*
Fr ∩ Ru	2	16	13.0208	1.2288	$2.12 \cdot 10^{-01}$
He ∩ Ru	2	26	13.0208	1.9968	$1.18 \cdot 10^{-04}$
He ∩ Fr	2	15	13.0208	1.1520	$3.11 \cdot 10^{-01}$
En ∩ Ru	2	19	13.0208	1.4592	$4.48 \cdot 10^{-02}$
En ∩ Fr	2	47	13.0208	3.6096	$3.12 \cdot 10^{-20}$
En ∩ He	2	13	13.0208	0.9984	$5.54 \cdot 10^{-01}$
De ∩ Ru	2	21	13.0208	1.6128	$1.14 \cdot 10^{-02}$
De ∩ Fr	2	37	13.0208	2.8416	$2.14 \cdot 10^{-11}$
De ∩ He	2	10	13.0208	0.7680	$8.71 \cdot 10^{-01}$
De ∩ En	2	38	13.0208	2.9184	$3.64 \cdot 10^{-12}$
He ∩ Fr ∩ Ru	3	5	1.6954	2.9491	$2.59 \cdot 10^{-02}$
En ∩ Fr ∩ Ru	3	10	1.6954	5.8982	$4.69 \cdot 10^{-06}$
En ∩ He ∩ Ru	3	5	1.6954	2.9491	$2.59 \cdot 10^{-02}$
En ∩ He ∩ Fr	3	9	1.6954	5.3084	$3.5 \cdot 10^{-05}$
De ∩ Fr ∩ Ru	3	11	1.6954	6.4881	$5.55 \cdot 10^{-07}$
De ∩ He ∩ Ru	3	4	1.6954	2.3593	$8.78 \cdot 10^{-02}$
De ∩ He ∩ Fr	3	4	1.6954	2.3593	$8.78 \cdot 10^{-02}$
De ∩ En ∩ Ru	3	10	1.6954	5.8982	$4.69 \cdot 10^{-06}$
De ∩ En ∩ Fr	3	24	1.6954	14.1558	$5.94 \cdot 10^{-23}$
De ∩ En ∩ He	3	5	1.6954	2.9491	$2.59 \cdot 10^{-02}$
En ∩ He ∩ Fr ∩ Ru	4	4	0.2208	18.1194	$6.82 \cdot 10^{-05}$
De ∩ He ∩ Fr ∩ Ru	4	4	0.2208	18.1194	$6.82 \cdot 10^{-05}$
De ∩ En ∩ Fr ∩ Ru	4	8	0.2208	36.2388	$4.28 \cdot 10^{-11}$
De ∩ En ∩ He ∩ Ru	4	4	0.2208	18.1194	$6.82 \cdot 10^{-05}$
De ∩ En ∩ He ∩ Fr	4	4	0.2208	18.1194	$6.82 \cdot 10^{-05}$
De ∩ En ∩ He ∩ Fr ∩ Ru	5	4	0.0287	139.1569	$2.13 \cdot 10^{-08}$

Table 9
Long-distance agreement condition (XLM-R, probeless).

Intersection	Degree	Obs. overlap	Exp. overlap	*FE*	*p*
Fr ∩ Ru	2	69	13.0208	5.2992	$3.46 \cdot 10^{-49}$
He ∩ Ru	2	53	13.0208	4.0704	$8.92 \cdot 10^{-27}$
He ∩ Fr	2	47	13.0208	3.6096	$3.12 \cdot 10^{-20}$
En ∩ Ru	2	61	13.0208	4.6848	$5.01 \cdot 10^{-37}$
En ∩ Fr	2	74	13.0208	5.6832	$6.89 \cdot 10^{-58}$
En ∩ He	2	35	13.0208	2.6880	$6.17 \cdot 10^{-10}$
De ∩ Ru	2	61	13.0208	4.6848	$5.01 \cdot 10^{-37}$
De ∩ Fr	2	68	13.0208	5.2224	$1.49 \cdot 10^{-47}$
De ∩ He	2	38	13.0208	2.9184	$3.64 \cdot 10^{-12}$
De ∩ En	2	69	13.0208	5.2992	$3.46 \cdot 10^{-49}$
He ∩ Fr ∩ Ru	3	40	1.6954	23.593	$1.36 \cdot 10^{-50}$
En ∩ Fr ∩ Ru	3	58	1.6954	34.2098	$1.77 \cdot 10^{-91}$
En ∩ He ∩ Ru	3	31	1.6954	18.2845	$4.77 \cdot 10^{-34}$
En ∩ He ∩ Fr	3	34	1.6954	20.054	$2.78 \cdot 10^{-39}$
De ∩ Fr ∩ Ru	3	56	1.6954	33.0301	$2.17 \cdot 10^{-86}$
De ∩ He ∩ Ru	3	33	1.6954	19.4642	$1.66 \cdot 10^{-37}$
De ∩ He ∩ Fr	3	33	1.6954	19.4642	$1.66 \cdot 10^{-37}$
De ∩ En ∩ Ru	3	52	1.6954	30.6709	$1.22 \cdot 10^{-76}$
De ∩ En ∩ Fr	3	62	1.6954	36.5691	$4.19 \cdot 10^{-102}$
De ∩ En ∩ He	3	29	1.6954	17.1049	$1.02 \cdot 10^{-30}$
En ∩ He ∩ Fr ∩ Ru	4	31	0.2208	140.4253	$2.94 \cdot 10^{-63}$
De ∩ He ∩ Fr ∩ Ru	4	31	0.2208	140.4253	$2.94 \cdot 10^{-63}$
De ∩ En ∩ Fr ∩ Ru	4	51	0.2208	231.0223	$1.99 \cdot 10^{-125}$
De ∩ En ∩ He ∩ Ru	4	27	0.2208	122.3059	$1.26 \cdot 10^{-52}$
De ∩ En ∩ He ∩ Fr	4	29	0.2208	131.3656	$7.23 \cdot 10^{-58}$
De ∩ En ∩ He ∩ Fr ∩ Ru	5	27	0.0287	939.3093	$5.53 \cdot 10^{-78}$

Appendix 3. Long-distance Condition Downsampled

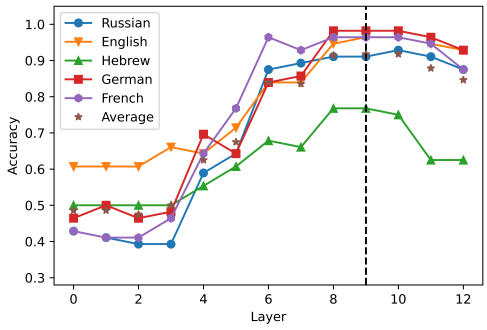

(a) Long-distance agreement, mBERT

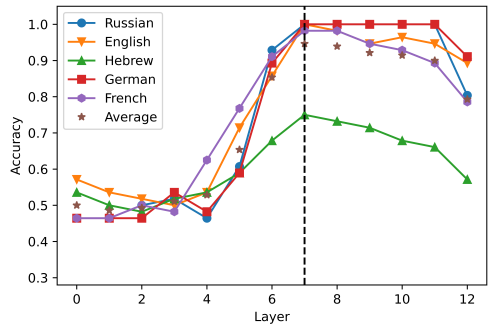

(b) Long-distance agreement, XLM-R

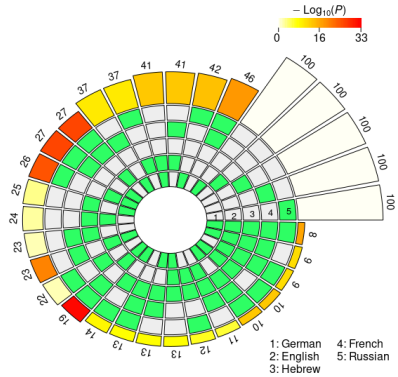

(c) Long-distance, layer 9, LCA, mBERT

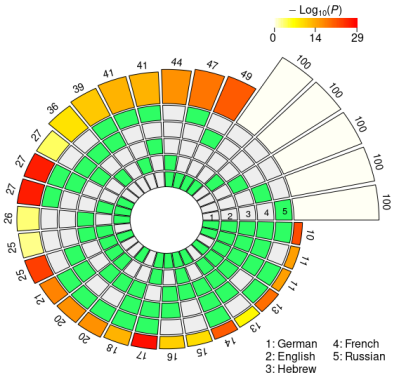

(d) Long-distance, layer 7, LCA, XLM-R

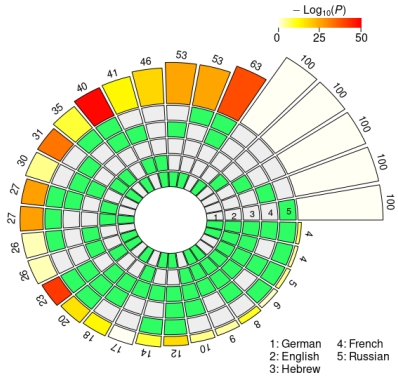

(e) Long-distance, layer 9, probeless, mBERT

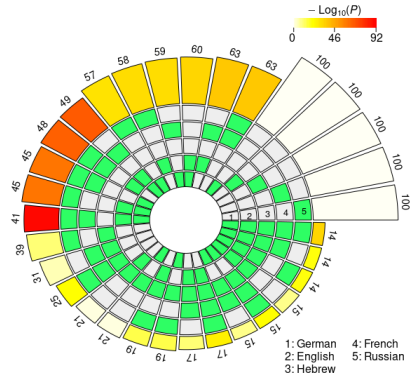

(f) Long-distance, layer 7, probeless, XLM-R

Figure 9
Layer-wise performance of the logistic classifier (top) and $N_{2\ldots5}$-way intersection statistics obtained with LCA (middle) and probeless ranking (bottom) on the downsampled long-distance agreement data.

In this section, we report the results we obtained by downsampling the long-distance condition to match the number of items available in the short-distance dataset—224 in the training (80%) and 56 in the test set (20%). Given the rather limited number of instances available in this condition, we decided to report in the article the results obtained with the larger dataset. Nonetheless, because we also comment on the short- vs. long-distance comparison, it is necessary to rule out the possible confound of the different amount of training data.[14] The peak of performance is obtained in the same layers as in the non-downsampled analyses (layers 9 and 7 for mBERT and XLM-R, respectively, see Figure 9a, 9b). The multi-set intersection analysis also shows a coherent pattern of results with respect to what we reported above. Indeed, in the case of mBERT the $N_{2\ldots4}$-way intersections with the highest *FE* are Fr ∩ Ru, Fr ∩ Ru ∩ (En ⊕ De), and Fr ∩ En ∩ De ∩ Ru, with Hebrew being absent in three combinations and French appearing in all of them (see Figure 9c, Table 10). Similarly, in the case of XLM-R the highest *FE* is obtained in De ∩ Fr, De ∩ Ru ∩ (En ⊕ Fr), and Fr ∩ En ∩ De ∩ Ru (Figure 9d, Table 11). Crucially, intersection sizes are consistently bigger in the downsampled long-distance condition (Figure 9c, 9d) than in the short-distance condition (Figure 3a,3a) across both model types.

Table 10
Downsampled long-distance condition, mBERT.

Intersection	Degree	Obs. overlap	Exp. overlap	*FE*	*p*
Fr ∩ Ru	2	46	13.0208	3.5328	$3.11 \cdot 10^{-19}$
He ∩ Ru	2	22	13.0208	1.6896	$5.20 \cdot 10^{-03}$
He ∩ Fr	2	23	13.0208	1.7664	$2.22 \cdot 10^{-03}$
En ∩ Ru	2	37	13.0208	2.8416	$2.14 \cdot 10^{-11}$
En ∩ Fr	2	41	13.0208	3.1488	$1.27 \cdot 10^{-14}$
En ∩ He	2	24	13.0208	1.8432	$8.90 \cdot 10^{-04}$
De ∩ Ru	2	42	13.0208	3.2256	$1.70 \cdot 10^{-15}$
De ∩ Fr	2	37	13.0208	2.8416	$2.14 \cdot 10^{-11}$
De ∩ He	2	25	13.0208	1.9200	$3.34 \cdot 10^{-04}$
De ∩ En	2	41	13.0208	3.1488	$1.27 \cdot 10^{-14}$
He ∩ Fr ∩ Ru	3	13	1.6954	7.6677	$5.51 \cdot 10^{-09}$
En ∩ Fr ∩ Ru	3	27	1.6954	15.9252	$1.64 \cdot 10^{-27}$
En ∩ He ∩ Ru	3	12	1.6954	7.0779	$5.84 \cdot 10^{-08}$
En ∩ He ∩ Fr	3	11	1.6954	6.4881	$5.54 \cdot 10^{-07}$
De ∩ Fr ∩ Ru	3	27	1.6954	15.9252	$1.64 \cdot 10^{-27}$
De ∩ He ∩ Ru	3	14	1.6954	8.2575	$4.68 \cdot 10^{-10}$
De ∩ He ∩ Fr	3	13	1.6954	7.6677	$5.51 \cdot 10^{-09}$
De ∩ En ∩ Ru	3	26	1.6954	15.3354	$5.85 \cdot 10^{-26}$
De ∩ En ∩ Fr	3	23	1.6954	13.5660	$1.69 \cdot 10^{-21}$
De ∩ En ∩ He	3	13	1.6954	7.6677	$5.51 \cdot 10^{-09}$
En ∩ He ∩ Fr ∩ Ru	4	9	0.2208	40.7686	$7.79 \cdot 10^{-13}$
De ∩ He ∩ Fr ∩ Ru	4	10	0.2208	45.2985	$1.23 \cdot 10^{-14}$
De ∩ En ∩ Fr ∩ Ru	4	19	0.2208	86.0671	$3.36 \cdot 10^{-33}$
De ∩ En ∩ He ∩ Ru	4	10	0.2208	45.2985	$1.23 \cdot 10^{-14}$
De ∩ En ∩ He ∩ Fr	4	9	0.2208	40.7686	$7.79 \cdot 10^{-13}$
De ∩ En ∩ He ∩ Fr ∩ Ru	5	8	0.0287	278.3139	$3.13 \cdot 10^{-18}$

14 We thank the anonymous reviewers for bringing this issue to our attention.

Table 11
Downsampled long-distance condition, XLM-R.

Intersection	Degree	Obs. overlap	Exp. overlap	*FE*	*p*
Fr ∩ Ru	2	54	13.0208	2.9952	$5.85 \cdot 10^{-13}$
He ∩ Ru	2	34	13.0208	3.1488	$1.27 \cdot 10^{-14}$
He ∩ Fr	2	30	13.0208	2.0736	$3.90 \cdot 10^{-05}$
En ∩ Ru	2	48	13.0208	3.1488	$1.27 \cdot 10^{-14}$
En ∩ Fr	2	48	13.0208	2.7648	$1.18 \cdot 10^{-10}$
En ∩ He	2	18	13.0208	1.9200	$3.34 \cdot 10^{-04}$
De ∩ Ru	2	54	13.0208	3.6096	$3.12 \cdot 10^{-20}$
De ∩ Fr	2	57	13.0208	3.7632	$2.62 \cdot 10^{-22}$
De ∩ He	2	26	13.0208	1.9968	$1.18 \cdot 10^{-04}$
De ∩ En	2	52	13.0208	3.3792	$2.59 \cdot 10^{-17}$
He ∩ Fr ∩ Ru	3	22	1.6954	10.6168	$9.22 \cdot 10^{-15}$
En ∩ Fr ∩ Ru	3	36	1.6954	12.3863	$1.07 \cdot 10^{-18}$
En ∩ He ∩ Ru	3	13	1.6954	11.7965	$2.39 \cdot 10^{-17}$
En ∩ He ∩ Fr	3	15	1.6954	7.6677	$5.50 \cdot 10^{-09}$
De ∩ Fr ∩ Ru	3	42	1.6954	15.9252	$1.64 \cdot 10^{-27}$
De ∩ He ∩ Ru	3	19	1.6954	11.7965	$2.39 \cdot 10^{-17}$
De ∩ He ∩ Fr	3	21	1.6954	9.4372	$2.50 \cdot 10^{-12}$
De ∩ En ∩ Ru	3	38	1.6954	15.9252	$1.64 \cdot 10^{-27}$
De ∩ En ∩ Fr	3	35	1.6954	14.7456	$1.94 \cdot 10^{-24}$
De ∩ En ∩ He	3	13	1.6954	8.8474	$3.59 \cdot 10^{-11}$
En ∩ He ∩ Fr ∩ Ru	4	12	0.2208	49.8283	$1.69 \cdot 10^{-16}$
De ∩ He ∩ Fr ∩ Ru	4	17	0.2208	63.4179	$2.09 \cdot 10^{-22}$
De ∩ En ∩ Fr ∩ Ru	4	30	0.2208	77.0074	$9.49 \cdot 10^{-29}$
De ∩ En ∩ He ∩ Ru	4	11	0.2208	58.8880	$2.19 \cdot 10^{-20}$
De ∩ En ∩ He ∩ Fr	4	12	0.2208	49.8283	$1.69 \cdot 10^{-16}$
De ∩ En ∩ He ∩ Fr ∩ Ru	5	10	0.0287	347.8924	$1.29 \cdot 10^{-23}$

Appendix 4. Pairwise Correlations in the Weight Matrices

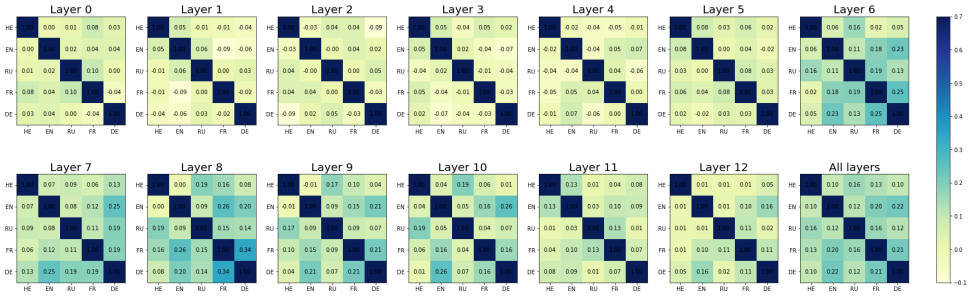

(a) Short-distance, mBERT

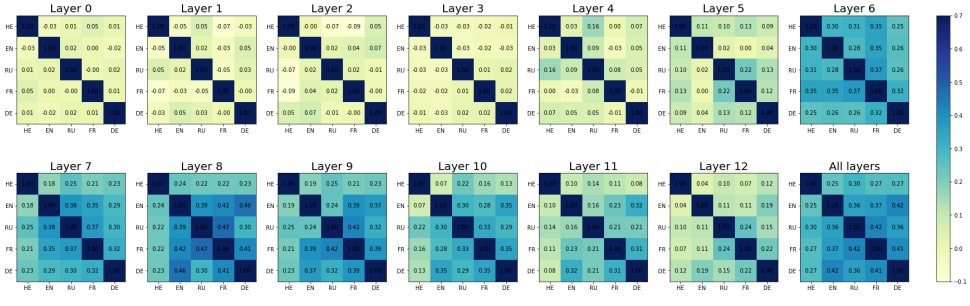

(b) Long-distance, mBERT

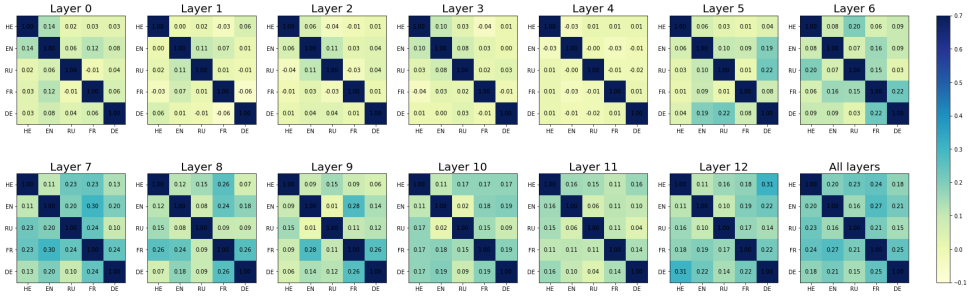

(c) Short-distance, XLM-R

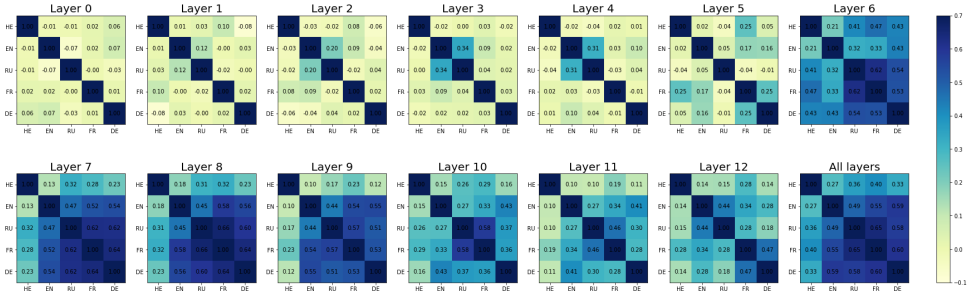

(d) Long-distance, XLM-R

Figure 10
Pairwise correlation coefficients between the weights learned by the classifiers, divided by layer, condition, and model type.

References

Abutalebi, Jubin, Stefano F. Cappa, and Daniela Perani. 2001. The bilingual brain as revealed by functional neuroimaging. *Bilingualism: Language and Cognition*, 4(2):179–190. https://doi.org/10.1017/S136672890100027X

Alain, Guillaume and Yoshua Bengio. 2016. Understanding intermediate layers using linear classifier probes. *arXiv preprint arXiv:1610.01644*.

Antverg, Omer and Yonatan Belinkov. 2021. On the pitfalls of analyzing individual neurons in language models. In *International Conference on Learning Representations*.

Bacon, Geoff and Terry Regier. 2019. Does BERT agree? Evaluating knowledge of structure dependence through agreement relations. *arXiv preprint arXiv:1908.09892*.

Bau, Anthony, Yonatan Belinkov, Hassan Sajjad, Nadir Durrani, Fahim Dalvi, and James Glass. 2018. Identifying and controlling important neurons in neural machine translation. In *International Conference on Learning Representations*.

Belinkov, Yonatan. 2022. Probing classifiers: Promises, shortcomings, and advances. *Computational Linguistics*, 48(1):207–219. https://doi.org/10.1162/coli_a_00422

Belinkov, Yonatan and James Glass. 2019. Analysis methods in neural language processing: A survey. *Transactions of the Association for Computational Linguistics*, 7:49–72. https://doi.org/10.1162/tacl_a_00254

Bernardy, Jean Philippe and Shalom Lappin. 2017. Using deep neural networks to learn syntactic agreement. *Linguistic Issues in Language Technology*. https://doi.org/10.33011/lilt.v15i.1413

Chi, Ethan A., John Hewitt, and Christopher D. Manning. 2020. Finding universal grammatical relations in multilingual BERT. In *Proceedings of the 58th Annual Meeting of the Association for Computational Linguistics*, pages 5564–5577. https://doi.org/10.18653/v1/2020.acl-main.493

Conneau, Alexis, Kartikay Khandelwal, Naman Goyal, Vishrav Chaudhary, Guillaume Wenzek, Francisco Guzmán, Édouard Grave, Myle Ott, Luke Zettlemoyer, and Veselin Stoyanov. 2020a. Unsupervised cross-lingual representation learning at scale. In *Proceedings of the 58th Annual Meeting of the Association for Computational Linguistics*, pages 8440–8451. https://doi.org/10.18653/v1/2020.acl-main.747

Conneau, Alexis, Shijie Wu, Haoran Li, Luke Zettlemoyer, and Veselin Stoyanov. 2020b. Emerging cross-lingual structure in pretrained language models. In *Proceedings of the 58th Annual Meeting of the Association for Computational Linguistics*, pages 6022–6034. https://doi.org/10.18653/v1/2020.acl-main.536

Cummins, Robert and George Schwarz. 1988. Radical connectionism. *The Southern Journal of Philosophy*, 26(5):43. https://doi.org/10.1111/j.2041-6962.1988.tb00462.x

Dalvi, Fahim, Nadir Durrani, Hassan Sajjad, Yonatan Belinkov, Anthony Bau, and James Glass. 2019a. What is one grain of sand in the desert? Analyzing individual neurons in deep NLP models. In *Proceedings of the AAAI Conference on Artificial Intelligence*, pages 6309–6317. https://doi.org/10.1609/aaai.v33i01.33016309

Dalvi, Fahim, Avery Nortonsmith, Anthony Bau, Yonatan Belinkov, Hassan Sajjad, Nadir Durrani, and James Glass. 2019b. Neurox: A toolkit for analyzing individual neurons in neural networks. In *Proceedings of the AAAI Conference on Artificial Intelligence*, pages 9851–9852. https://doi.org/10.1609/aaai.v33i01.33019851

Dalvi, Fahim, Hassan Sajjad, Nadir Durrani, and Yonatan Belinkov. 2020. Analyzing redundancy in pretrained transformer models. In *Proceedings of the 2020 Conference on Empirical Methods in Natural Language Processing (EMNLP)*, pages 4908–4926. https://doi.org/10.18653/v1/2020.emnlp-main.398

Del, Maksym and Mark Fishel. 2021. Establishing interlingua in multilingual language models. *ArXiv*, abs/2109.01207.

Devlin, Jacob, Ming-Wei Chang, Kenton Lee, and Kristina Toutanova. 2019. BERT: Pre-training of deep bidirectional transformers for language understanding. In *Proceedings of the 2019 Conference of the North American Chapter of the Association for Computational Linguistics: Human Language Technologies, Volume 1 (Long and Short Papers)*, pages 4171–4186.

Dhar, Prajit and Arianna Bisazza. 2021. Understanding cross-lingual syntactic transfer in multilingual recurrent neural networks. In *Proceedings of the 23rd Nordic Conference on Computational Linguistics (NoDaLiDa)*, pages 74–85.

Doddapaneni, Sumanth, Gowtham Ramesh, Anoop Kunchukuttan, Pratyush Kumar,

and Mitesh M. Khapra. 2021. A primer on pretrained multilingual language models. *arXiv preprint arXiv:2107.00676*.

Dufter, Philipp and Hinrich Schütze. 2020. Identifying necessary elements for BERT's multilinguality. *arXiv preprint arXiv:2005.00396*. https://doi.org/10.18653/v1/2020.emnlp-main.358

Finlayson, Matthew, Aaron Mueller, Sebastian Gehrmann, Stuart Shieber, Tal Linzen, and Yonatan Belinkov. 2021. Causal analysis of syntactic agreement mechanisms in neural language models. In *Proceedings of the 59th Annual Meeting of the Association for Computational Linguistics and the 11th International Joint Conference on Natural Language Processing (Volume 1: Long Papers)*, pages 1828–1843. https://doi.org/10.18653/v1/2021.acl-long.144

Goldberg, Yoav. 2019. Assessing BERT's syntactic abilities. *CoRR*, abs/1901.05287.

Gonen, Hila, Shauli Ravfogel, and Yoav Goldberg. 2022. Analyzing gender representation in multilingual models. In *Proceedings of the 7th Workshop on Representation Learning for NLP*, pages 67–77. https://doi.org/10.18653/v1/2022.repl4nlp-1.8

Green, David W. 2008. Bilingual aphasia: Adapted language networks and their control. *Annual Review of Applied Linguistics*, 28:25–48. https://doi.org/10.1017/S0267190508080057

Guarasci, Raffaele, Stefano Silvestri, Giuseppe De Pietro, Hamido Fujita, and Massimo Esposito. 2022. BERT syntactic transfer: A computational experiment on Italian, French and English languages. *Computer Speech & Language*, 71:101261. https://doi.org/10.1016/j.csl.2021.101261

Gulordava, Kristina, Piotr Bojanowski, Édouard Grave, Tal Linzen, and Marco Baroni. 2018. Colorless green recurrent networks dream hierarchically. In *Proceedings of the 2018 Conference of the North American Chapter of the Association for Computational Linguistics: Human Language Technologies, Volume 1 (Long Papers)*, pages 1195–1205. https://doi.org/10.18653/v1/N18-1108

Jawahar, Ganesh, Benoît Sagot, and Djamé Seddah. 2019. What does BERT learn about the structure of language? In *Proceedings of the 57th Annual Meeting of the Association for Computational Linguistics*, pages 3651–3657. https://doi.org/10.18653/v1/P19-1356

Joshi, Pratik, Sebastin Santy, Amar Budhiraja, Kalika Bali, and Monojit Choudhury. 2020. The state and fate of linguistic diversity and inclusion in the NLP world. In *Proceedings of the 58th Annual Meeting of the Association for Computational Linguistics*, pages 6282–6293. https://doi.org/10.18653/v1/2020.acl-main.560

Karpathy, Andrej, Justin Johnson, and Li Fei-Fei. 2015. Visualizing and understanding recurrent networks. *arXiv preprint arXiv:1506.02078*.

Karthikeyan, K., Wang Zihan, Stephen Mayhew, and Dan Roth. 2020. Cross-lingual ability of multilingual BERT: An empirical study. In *International Conference on Learning Representations*.

Kementchedjhieva, Yova and Adam Lopez. 2018. 'Indicatements' that character language models learn English morpho-syntactic units and regularities. In *Proceedings of the 2018 EMNLP Workshop BlackboxNLP: Analyzing and Interpreting Neural Networks for NLP*, pages 145–153. https://doi.org/10.18653/v1/W18-5417

Kim, Karl H. S., Norman R. Relkin, Kyoung-Min Lee, and Joy Hirsch. 1997. Distinct cortical areas associated with native and second languages. *Nature*, 388(6638):171–174. https://doi.org/10.1038/40623, PubMed: 9217156

Klein, Stav and Reut Tsarfaty. 2020. Getting the ##life out of living: How adequate are word-pieces for modelling complex morphology? In *Proceedings of the 17th SIGMORPHON Workshop on Computational Research in Phonetics, Phonology, and Morphology*, pages 204–209. https://doi.org/10.18653/v1/2020.sigmorphon-1.24

Kuncoro, Adhiguna, Chris Dyer, John Hale, Dani Yogatama, Stephen Clark, and Phil Blunsom. 2018. LSTMs can learn syntax-sensitive dependencies well, but modeling structure makes them better. In *Proceedings of the 56th Annual Meeting of the Association for Computational Linguistics (Volume 1: Long Papers)*, pages 1426–1436. https://doi.org/10.18653/v1/P18-1132

Lakretz, Yair, Germán Kruszewski, Theo Desbordes, Dieuwke Hupkes, Stanislas Dehaene, and Marco Baroni. 2019. The emergence of number and syntax units in LSTM language models. In *Proceedings of NAACL-HLT*, pages 11–20. https://doi.org/10.18653/v1/N19-1002

Lasri, Karim, Alessandro Lenci, and Thierry Poibeau. 2022. Does BERT really agree? Fine-grained analysis of lexical dependence on a syntactic task. In *Findings*

of the Association for Computational Linguistics: ACL 2022, pages 2309–2315. https://doi.org/10.18653/v1/2022.findings-acl.181

Lauscher, Anne, Vinit Ravishankar, Ivan Vulić, and Goran Glavaš. 2020. From zero to hero: On the limitations of zero-shot language transfer with multilingual Transformers. In *Proceedings of the 2020 Conference on Empirical Methods in Natural Language Processing (EMNLP)*, pages 4483–4499. https://doi.org/10.18653/v1/2020.emnlp-main.363

Li, Jiwei, Xinlei Chen, Eduard Hovy, and Dan Jurafsky. 2015. Visualizing and understanding neural models in NLP. *arXiv preprint arXiv:1506.01066*. https://doi.org/10.18653/v1/N16-1082

Linzen, Tal, Emmanuel Dupoux, and Yoav Goldberg. 2016. Assessing the ability of LSTMs to learn syntax-sensitive dependencies. *Transactions of the Association for Computational Linguistics*, 4:521–535. https://doi.org/10.1162/tacl_a_00115

Liu, Zihan, Genta Indra Winata, Andrea Madotto, and Pascale Fung. 2020. Exploring fine-tuning techniques for pre-trained cross-lingual models via continual learning. *arXiv preprint arXiv:2004.14218*.

Marvin, Rebecca and Tal Linzen. 2018. Targeted syntactic evaluation of language models. In *Proceedings of the 2018 Conference on Empirical Methods in Natural Language Processing*, pages 1192–1202. https://doi.org/10.18653/v1/D18-1151

McCloskey, Michael. 1991. Networks and theories: The place of connectionism in cognitive science. *Psychological Science*, 2(6):387–395. https://doi.org/10.1111/j.1467-9280.1991.tb00173.x

Mueller, Aaron, Garrett Nicolai, Panayiota Petrou-Zeniou, Natalia Talmina, and Tal Linzen. 2020. Cross-linguistic syntactic evaluation of word prediction models. In *Proceedings of the 58th Annual Meeting of the Association for Computational Linguistics*, pages 5523–5539. https://doi.org/10.18653/v1/2020.acl-main.490

Muller, Benjamin, Yanai Elazar, Benoît Sagot, and Djamé Seddah. 2021. First align, then predict: Understanding the cross-lingual ability of multilingual BERT. In *Proceedings of the 16th Conference of the European Chapter of the Association for Computational Linguistics: Main Volume*, pages 2214–2231. https://doi.org/10.18653/v1/2021.eacl-main.189

Perani, Daniela and Jubin Abutalebi. 2005. The neural basis of first and second language processing. *Current Opinion in Neurobiology*, 15(2):202–206. https://doi.org/10.1016/j.conb.2005.03.007, PubMed: 15831403

Perani, Daniela, Eraldo Paulesu, Nuria Sebastian Galles, Emmanuel Dupoux, Stanislas Dehaene, Valentino Bettinardi, Stefano F. Cappa, Ferruccio Fazio, and Jacques Mehler. 1998. The bilingual brain. Proficiency and age of acquisition of the second language. *Brain: A Journal of Neurology*, 121(10):1841–1852. https://doi.org/10.1093/brain/121.10.1841, PubMed: 9798741

Pinter, Yuval, Marc Marone, and Jacob Eisenstein. 2019. Character eyes: Seeing language through character-level taggers. In *Proceedings of the 2019 ACL Workshop BlackboxNLP: Analyzing and Interpreting Neural Networks for NLP*, pages 95–102. https://doi.org/10.18653/v1/W19-4811

Pires, Telmo, Eva Schlinger, and Dan Garrette. 2019. How multilingual is multilingual BERT? In *Proceedings of the 57th Annual Meeting of the Association for Computational Linguistics*, pages 4996–5001. https://doi.org/10.18653/v1/P19-1493

Radford, Alec, Rafal Jozefowicz, and Ilya Sutskever. 2017. Learning to generate reviews and discovering sentiment. *arXiv preprint arXiv:1704.01444*.

Serrano, Sofia and Noah A. Smith. 2019. Is attention interpretable? In *Proceedings of the 57th Annual Meeting of the Association for Computational Linguistics*, pages 2931–2951. https://doi.org/10.18653/v1/P19-1282

Singh, Jasdeep, Bryan McCann, Richard Socher, and Caiming Xiong. 2019. BERT is not an interlingua and the bias of tokenization. In *Proceedings of the 2nd Workshop on Deep Learning Approaches for Low-Resource NLP (DeepLo 2019)*, pages 47–55. https://doi.org/10.18653/v1/D19-6106

Stanczak, Karolina, Edoardo Ponti, Lucas Torroba Hennigen, Ryan Cotterell, and Isabelle Augenstein. 2022. Same neurons, different languages: Probing morphosyntax in multilingual pre-trained models. In *Proceedings of the 2022 Conference of the North American Chapter of the Association for Computational Linguistics: Human Language Technologies*, pages 1589–1598. https://doi.org/10.18653/v1/2022.naacl-main.114

Tan, Li Hai, Lin Chen, Virginia Yip, Alice H. D. Chan, Jing Yang, Jia-Hong Gao, and

Wai Ting Siok. 2011. Activity levels in the left hemisphere caudate–fusiform circuit predict how well a second language will be learned. *Proceedings of the National Academy of Sciences*, 108(6):2540–2544. https://doi.org/10.1073/pnas.0909623108, PubMed: 21262807

Tang, Zhiyuan, Ying Shi, Dong Wang, Yang Feng, and Shiyue Zhang. 2017. Memory visualization for gated recurrent neural networks in speech recognition. In *2017 IEEE International Conference on Acoustics, Speech and Signal Processing (ICASSP)*, pages 2736–2740. https://doi.org/10.1109/ICASSP.2017.7952654

Tham, Wendy W. P., Susan J. Rickard Liow, Jagath C. Rajapakse, Tan Choong Leong, Samuel E. S. Ng, Winston E. H. Lim, and Lynn G. Ho. 2005. Phonological processing in Chinese-English bilingual biscriptals: An fMRI study. *NeuroImage*, 28(3):579–587. https://doi.org/10.1016/j.neuroimage.2005.06.057, PubMed: 16126414

van Schijndel, Marten, Aaron Mueller, and Tal Linzen. 2019. Quantity doesn't buy quality syntax with neural language models. In *Proceedings of the 2019 Conference on Empirical Methods in Natural Language Processing and the 9th International Joint Conference on Natural Language Processing (EMNLP-IJCNLP)*, pages 5831–5837. https://doi.org/10.18653/v1/D19-1592

Wang, Minghui, Yongzhong Zhao, and Bin Zhang. 2015. Efficient test and visualization of multi-set intersections. *Scientific Reports*, 5:16923. https://doi.org/10.1038/srep16923, PubMed: 26603754

Wu, Shijie and Mark Dredze. 2019. Beto, bentz, becas: The surprising cross-lingual effectiveness of BERT. In *Proceedings of the 2019 Conference on Empirical Methods in Natural Language Processing and the 9th International Joint Conference on Natural Language Processing (EMNLP-IJCNLP)*, pages 833–844. https://doi.org/10.18653/v1/D19-1077

Wu, Shijie and Mark Dredze. 2020. Are all languages created equal in multilingual BERT? In *Proceedings of the 5th Workshop on Representation Learning for NLP*, pages 120–130. https://doi.org/10.18653/v1/2020.repl4nlp-1.16

Xu, Min, Daniel Baldauf, Chun Qi Chang, Robert Desimone, and Li Hai Tan. 2017. Distinct distributed patterns of neural activity are associated with two languages in the bilingual brain. *Science Advances*, 3(7):e1603309. https://doi.org/10.1126/sciadv.1603309, PubMed: 28706990

Zou, Hui and Trevor Hastie. 2005. Regularization and variable selection via the elastic net. *Journal of the Royal Statistical Society: Series B (Statistical Methodology)*, 67(2):301–320. https://doi.org/10.1111/j.1467-9868.2005.00503.x

Zuckermann, Ghil'ad. 2006. A new vision for Israeli Hebrew: Theoretical and practical implications of analyzing Israel's main language as a semi-engineered Semito-European hybrid language. *Journal of Modern Jewish Studies*, 5(1):57–71. https://doi.org/10.1080/14725880500511175